

LHC 750 GeV Diphoton excess in a radiative seesaw model

Shinya Kanemura,^a Kenji Nishiwaki,^b Hiroshi Okada,^c
Yuta Orikasa,^d Seong Chan Park,^e Ryoutaro Watanabe^f

^a *Department of Physics, University of Toyama,
3190 Gofuku, Toyama 930-8555, Japan*

^{b,d,e} *School of Physics, Korea Institute for Advanced Study,
Seoul 02455, Republic of Korea*

^c *Physics Division, National Center for Theoretical Sciences,
National Tsing-Hua University, Hsinchu 30013, Taiwan*

^d *Department of Physics and Astronomy, Seoul National University,
Seoul 151-742, Republic of Korea*

^e *Department of Physics and IPAP, Yonsei University,
Seoul 03722, Republic of Korea*

^f *Center for Theoretical Physics of the Universe,
Institute for Basic Science (IBS), Daejeon, 34051, Republic of Korea*

15 February 2019

Abstract

We investigate a possibility for explaining the recently announced 750 GeV diphoton excess by the ATLAS and the CMS experiments at the CERN LHC in a model with multiple doubly-charged particles, which was originally suggested for explaining tiny neutrino masses through a three-loop effect in a natural way. The enhanced radiatively generated effective coupling of a new singlet scalar S with diphoton, with multiple charged particles in the loop, enlarges the production rate of S in $pp \rightarrow S + X$ via photon fusion process and also the decay width $\Gamma(S \rightarrow \gamma\gamma)$ even without assuming a tree level production mechanism. Very interestingly, we find that the branching ratio $\mathcal{B}(S \rightarrow \gamma\gamma)$ is $\simeq 60\%$ fixed by quantum numbers and the model is consistent with all the constraints from 8 TeV LHC data.

^a E-mail: kanemu@sci.u-toyama.ac.jp

^b E-mail: nishiken@kias.re.kr

^c E-mail: macokada3hiroshi@gmail.com

^d E-mail: orikasa@kias.re.kr

^e E-mail: sc.park@yonsei.ac.kr

^f E-mail: wryou1985@ibs.re.kr

1 Introduction

Very recently, both of the ATLAS and CMS experiments announced the observation of a new resonance around 750 GeV as a bump in the diphoton invariant mass spectrum from the run-II data in $\sqrt{s} = 13$ TeV [1, 2]. Their results are based on the accumulated data of 3.2 fb^{-1} (ATLAS) and 2.6 fb^{-1} (CMS), and local/global significances are $3.9\sigma/2.3\sigma$ (ATLAS) and $2.6\sigma/\lesssim 1.2\sigma$ (CMS), respectively. The best-fit values of the invariant mass are 750 GeV by ATLAS and 760 GeV by CMS, where the ATLAS also reported the best-fit value of the total width as 45 GeV. After the advent of the announcement, various ways for explaining the 750 GeV excess have been proposed in Refs. [3–120]. An interpretation of the excess in terms of the signal strength of a scalar (or a pseudoscalar) resonance S , $pp \rightarrow S + X \rightarrow \gamma\gamma + X$, was done in Ref. [9] based on the expected and observed exclusion limits. The authors claimed,

$$\mu_{13\text{TeV}}^{\text{ATLAS}} = \sigma(pp \rightarrow S + X)_{13\text{TeV}} \times \mathcal{B}(S \rightarrow \gamma\gamma) = (6.2^{+2.4}_{-2.0}) \text{ fb}, \quad (1.1)$$

$$\mu_{13\text{TeV}}^{\text{CMS}} = \sigma(pp \rightarrow S + X)_{13\text{TeV}} \times \mathcal{B}(S \rightarrow \gamma\gamma) = (5.6 \pm 2.4) \text{ fb}, \quad (1.2)$$

with a Poissonian likelihood function (for the ATLAS measurement) and the Gaussian approximation (for the CMS measurement), respectively.

On the other hand, both of the ATLAS and CMS groups reported that no significant excess over the standard model (SM) background was observed in their analyses based on the run-I data at $\sqrt{s} = 8$ TeV [121, 122], while a mild upward bump was found in their data around 750 GeV. In Ref. [9], the signal strengths at $\sqrt{s} = 8$ TeV were extracted by use of the corresponding expected and observed exclusion limits given by the experiments, in the Gaussian approximation, as

$$\mu_{8\text{TeV}}^{\text{ATLAS}} = \sigma(pp \rightarrow S + X)_{8\text{TeV}} \times \mathcal{B}(S \rightarrow \gamma\gamma) = (0.46 \pm 0.85) \text{ fb}, \quad (1.3)$$

$$\mu_{8\text{TeV}}^{\text{CMS}} = \sigma(pp \rightarrow S + X)_{8\text{TeV}} \times \mathcal{B}(S \rightarrow \gamma\gamma) = (0.63 \pm 0.25) \text{ fb}. \quad (1.4)$$

It is mentioned that when we upgrade the collider energy from 8 TeV to 13 TeV, a factor 4.7 enhancement is expected [9, 123], when the resonant particle is produced via gluon fusion, and then the data at $\sqrt{s} = 8$ TeV and 13 TeV are compatible at around 2σ confidence level (C.L.). These observations would give us a stimulating hint for surveying the structure of physics beyond the SM above the electroweak scale even though the accumulated amount of the data would not be enough for detailed discussions and the errors are large at the present stage.

A key point to understand the resonance is the fact that no bump around 750 GeV has been found in the other final states in both of the 8 TeV and 13 TeV data. If $\mathcal{B}(S \rightarrow \gamma\gamma)$ is the same as the 750 GeV Higgs one, $\mathcal{B}(h \rightarrow \gamma\gamma)|_{750 \text{ GeV SM}} = 1.79 \times 10^{-7}$ [124], we can immediately recognize that such a possibility is inconsistent with the observed results, e.g., in ZZ final state, at $\sqrt{s} = 8$ TeV, where the experimental 95% C.L. limits on the ZZ channel are 22 fb by ATLAS [125], 27 fb by CMS [126], and the branching ratio $\mathcal{B}(h \rightarrow ZZ)|_{750 \text{ GeV SM}} = 0.290$ [124]. In general, the process $S \rightarrow \gamma\gamma$ should be loop induced since S has zero electromagnetic charge and then the value of $\mathcal{B}(S \rightarrow \gamma\gamma)$ tends to be suppressed because tree level decay branches generate primary components of the total width of S . Then, a reasonable setup for explaining the resonance consistently is that all of the decay channels of S are one loop induced, where S would be a gauge singlet under $SU(3)_C$ and $SU(2)_L$ since a non-singlet gauge assignment leads to a tree level gauge interaction.

An example of this direction is that S is a singlet scalar and it couples to vector-like quarks, which contribute to both of $pp \rightarrow S + X$ and $S \rightarrow \gamma\gamma$ via gluon fusion and photon fusion, respectively. In such a possibility, a typical digit of $\mathcal{B}(S \rightarrow \gamma\gamma)$ is $\sim 1\%$. On the other hand, when $\mathcal{B}(S \rightarrow \gamma\gamma)$ is $\mathcal{O}(10)\%$, another direction for generating S at the one loop level opens up

via photon fusion discussed in Refs. [32, 38]. When a model contains $SU(2)_L$ singlet particles with large $U(1)_Y$ hypercharges, the magnitude of the photon fusions in the production and decay sequences is enhanced and we can accommodate the 750 GeV excess.

In this paper, we focus on the radiative seesaw models [127–131], especially where neutrino masses are generated at the three loop level [132–149]. In such type of scenarios, multiple charged scalars are introduced for realizing three-loop origin of the neutrino mass, (distinctively from the models with one or two loops). We show that when these charged scalars couple to the singlet S strongly enough, we can achieve a reasonable amount of the production cross section in $pp \rightarrow S + X \rightarrow \gamma\gamma + X$ through photon fusion. Concretely, we start from the three loop model [146], and extend the model with additional charged scalars to explain the data.

This paper is organized as follows. In Sec. 2, we introduce our model based on the model for three-loop induced neutrino masses. In Sec. 3, we show detail of analysis and numerical results. In Sec. 4, we are devoted to summary and discussions.

2 Model

Multiple (doubly) charged particles would induce a large radiative coupling with a singlet scalar S with $\gamma\gamma$ via one-loop diagrams. We may find the source from multi-Higgs models or extra dimensions [150–167] but here we focus on a model for radiative neutrino masses recently suggested by some of the authors [146] as a benchmark model, which can be extended with a singlet scalar S for the 750 GeV resonance.

2.1 Review: A model for three-loop induced neutrino mass

Our strategy is based on the three loop induced radiative neutrino model with a $U(1)$ global symmetry [146], where we introduce three Majorana fermions $N_{R1,2,3}$ and new bosons; one gauge-singlet neutral boson Σ_0 , two singly charged singlet scalars (h_1^\pm, h_2^\pm), and one gauge-singlet doubly charged boson $k^{\pm\pm}$ to the SM. The particle contents and their charges are shown in Table 1.

	Lepton Fields			Scalar Fields					New Scalar Fields	
Characters	L_{Li}	e_{Ri}	N_{Ri}	Φ	Σ_0	h_1^+	h_2^+	k^{++}	j_a^{++}	S
$SU(3)_C$	1	1	1	1	1	1	1	1	1	1
$SU(2)_L$	2	1	1	2	1	1	1	1	1	1
$U(1)_Y$	$-1/2$	-1	0	$1/2$	0	1	1	2	2	0
$U(1)$	0	0	$-x$	0	$2x$	0	x	$2x$	$2x$	0

Table 1: Contents of lepton and scalar fields and their charge assignment under $SU(3)_C \times SU(2)_L \times U(1)_Y \times U(1)$, where $U(1)$ is an additional global symmetry and $x \neq 0$. The subscripts found in the lepton fields i ($= 1, 2, 3$) indicate generations of the fields. The bold letters emphasize that these numbers correspond to representations of the Lie groups of the NonAbelian gauge interactions. The scalar particles shown in the right category (New Scalar Fields) are added to the original model proposed in Ref. [146] to explain the 750 GeV excess.

We assume that only the SM-like Higgs Φ and the additional neutral scalar Σ_0 have VEVs, which are symbolized as $\langle \Phi \rangle \equiv v/\sqrt{2}$ and $\langle \Sigma_0 \rangle \equiv v'/\sqrt{2}$, respectively. x ($\neq 0$) is an arbitrary number of the charge of the hidden $U(1)$ symmetry, and under the assignments, neutrino mass matrix is generated at the three loop level, where a schematic picture is shown in Fig. 1. Note

that a remnant Z_2 symmetry remains after the hidden $U(1)$ symmetry breaking and the particles $N_{R1,2,3}$ and h_2^\pm have negative parities. Then, when a Majorana neutrino is the lightest among them, it becomes a dark matter (DM) candidate and the stability is accidentally ensured.

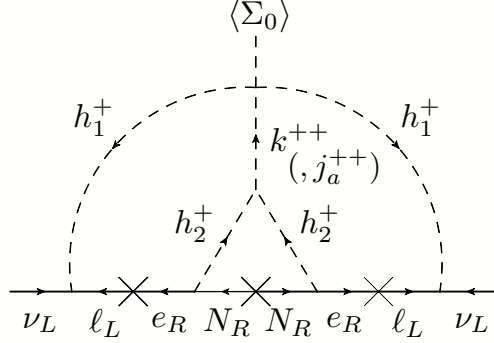


Figure 1: A schematic description for the radiative generation of neutrino masses.

In the original model, the Lagrangian of Yukawa sector \mathcal{L}_Y and scalar potential \mathcal{V} , allowed under the gauge and global symmetries, are given as

$$-\mathcal{L}_Y = (y_\ell)_{ij} \bar{L}_{Li} \Phi e_{Rj} + \frac{1}{2} (y_L)_{ij} \bar{L}_{Li}^c L_{Lj} h_1^+ + (y_R)_{ij} \bar{N}_{Ri} e_{Rj}^c h_2^- + \frac{1}{2} (y_N)_{ij} \Sigma_0 \bar{N}_{Ri}^c N_{Rj} + \text{h.c.}, \quad (2.1)$$

$$\begin{aligned} \mathcal{V} = & m_\Phi^2 |\Phi|^2 + m_\Sigma^2 |\Sigma_0|^2 + m_{h_1}^2 |h_1^+|^2 + m_{h_2}^2 |h_2^+|^2 + m_k^2 |k^{++}|^2 \\ & + \left[\lambda_{11} \Sigma_0^* h_1^- h_1^- k^{++} + \mu_{22} h_2^+ h_2^+ k^{--} + \text{h.c.} \right] + \lambda_\Phi |\Phi|^4 + \lambda_{\Phi\Sigma} |\Phi|^2 |\Sigma_0|^2 + \lambda_{\Phi h_1} |\Phi|^2 |h_1^+|^2 \\ & + \lambda_{\Phi h_2} |\Phi|^2 |h_2^+|^2 + \lambda_{\Phi k} |\Phi|^2 |k^{++}|^2 + \lambda_\Sigma |\Sigma_0|^4 + \lambda_{\Sigma h_1} |\Sigma_0|^2 |h_1^+|^2 + \lambda_{\Sigma h_2} |\Sigma_0|^2 |h_2^+|^2 \\ & + \lambda_{\Sigma k} |\Sigma_0|^2 |k^{++}|^2 + \lambda_{h_1} |h_1^+|^4 + \lambda_{h_1 h_2} |h_1^+|^2 |h_2^+|^2 + \lambda_{h_1 k} |h_1^+|^2 |k^{++}|^2 \\ & + \lambda_{h_2} |h_2^+|^4 + \lambda_{h_2 k} |h_2^+|^2 |k^{++}|^2 + \lambda_k |k^{++}|^4, \end{aligned} \quad (2.2)$$

where the indices i, j indicate matter generations and the superscript “ c ” means charge conjugation (with the $SU(2)_L$ rotation by $i\sigma_2$ for $SU(2)_L$ doublets). We assume that y_N is diagonal, where the right-handed neutrino masses are calculated as $M_{N_i} = \frac{v'}{\sqrt{2}} (y_N)_{ii}$ with the assumed ordering $M_{N_1} (= \text{DM mass}) < M_{N_2} < M_{N_3}$. The neutral scalar fields are shown in the Unitary gauge as

$$\Phi = \begin{bmatrix} 0 \\ \frac{v+\phi}{\sqrt{2}} \end{bmatrix}, \quad \Sigma_0 = \frac{v' + \sigma}{\sqrt{2}} e^{iG/v'}, \quad (2.3)$$

with $v \simeq 246$ GeV and an associated Nambu-Goldstone (NG) boson G via the global $U(1)$ breaking due to the occurrence of nonzero v' . Requiring the tadpole conditions, $\partial\mathcal{V}/\partial\phi|_{\phi=v} = \partial\mathcal{V}/\partial\sigma|_{\sigma=v'} = 0$, the resultant mass matrix squared of the CP even components (ϕ, σ) is given by

$$m^2(\phi, \sigma) = \begin{bmatrix} 2\lambda_\Phi v^2 & \lambda_{\Phi\Sigma} v v' \\ \lambda_{\Phi\Sigma} v v' & 2\lambda_\Sigma v'^2 \end{bmatrix} = \begin{bmatrix} \cos \alpha & \sin \alpha \\ -\sin \alpha & \cos \alpha \end{bmatrix} \begin{bmatrix} m_h^2 & 0 \\ 0 & m_H^2 \end{bmatrix} \begin{bmatrix} \cos \alpha & -\sin \alpha \\ \sin \alpha & \cos \alpha \end{bmatrix}, \quad (2.4)$$

where h is the SM-like Higgs ($m_h = 125$ GeV) and H is an additional CP even Higgs mass eigenstate. The mixing angle α is determined as

$$\sin 2\alpha = \frac{2\lambda_{\Phi\Sigma} v v'}{m_H^2 - m_h^2}. \quad (2.5)$$

The neutral bosons ϕ and σ are represented in terms of the mass eigenstates h and H as

$$\phi = h \cos \alpha + H \sin \alpha, \quad \sigma = -h \sin \alpha + H \cos \alpha. \quad (2.6)$$

Note that the two CP even scalars h and H works as DM-portal scalars and play a significant role in the DM pair annihilation. The mass eigenvalues for the singly charged bosons h_1^\pm , h_2^\pm and the doubly charged boson $k^{\pm\pm}$ are given as

$$\begin{aligned} m_{h_1^\pm}^2 &= m_{h_1}^2 + \frac{1}{2}(\lambda_{\Phi h_1} v^2 + \lambda_{\Sigma h_1} v'^2), & m_{h_2^\pm}^2 &= m_{h_2}^2 + \frac{1}{2}(\lambda_{\Phi h_2} v^2 + \lambda_{\Sigma h_2} v'^2), \\ m_{k^{\pm\pm}}^2 &= m_k^2 + \frac{1}{2}(\lambda_{\Phi k} v^2 + \lambda_{\Sigma k} v'^2). \end{aligned} \quad (2.7)$$

This model can explain the smallness of the observed neutrino masses and the presence of DM without severe parameter tuning. A summary of the features in the model is given in Appendix.

Here we introduce a real singlet scalar S in the model and assume that it couples with the doubly charged scalar(s). Due to the contributions of the charged particles in the loop, a large branching ratio $\mathcal{B}(S \rightarrow \gamma\gamma)$ is achievable without assuming tree level interactions [32, 38]. When $\mathcal{B}(S \rightarrow \gamma\gamma)$ is sizable, the production cross section of the resonance particle, $\sigma(pp \rightarrow S + X)$, becomes large through photon fusion processes thus we don't have to rely on gluon fusion processes, which often requests additional colored particles that brings in dangerous hadronic activities. Thus we may explain the 750 GeV excess as pointed out in [32, 38].

2.2 Extension with a scalar S for the 750 GeV resonance

In the following part, we consider an extension of the original model with the new interactions as

$$\begin{aligned} \Delta\mathcal{V} &= \hat{\mu}_{Sk} S |k^{++}|^2 + \hat{\lambda}_{Sk} S^2 |k^{++}|^2 + \mathcal{V}(S) \\ &+ \sum_{a=1}^{N_j} \left\{ \hat{m}_{j_a^{\pm\pm}}^2 |j_a^{++}|^2 + \hat{\mu}_{Sj_a} S |j_a^{++}|^2 + \hat{\lambda}_{Sj_a} S^2 |j_a^{++}|^2 + \left[\lambda_{11}^{(a)} \Sigma_0^* h_1^- h_1^- j_a^{++} + \mu_{22}^{(a)} h_2^+ h_2^+ j_a^{--} + \text{h.c.} \right] \right\}, \end{aligned} \quad (2.8)$$

where S is a real scalar and $j_a^{\pm\pm}$ ($a = 1, 2, \dots, N_j$) are additional $SU(2)_L$ singlet doubly charged scalars with hyper charge +2 and a global $U(1)$ charge $+2x$. $\mathcal{V}(S)$ represents the potential of the singlet scalar S . Here, we assume that S has a VEV, and S should be replaced as $S \rightarrow \langle S \rangle + S$. After the replacement, we pick up the relevant terms for our analysis and summarize,

$$\begin{aligned} \Delta\mathcal{V}_{\text{eff}} &= \mu_{Sk} S |k^{++}|^2 + \frac{1}{2} m_S^2 S^2 \\ &+ \sum_{a=1}^{N_j} \left\{ m_{j_a^{\pm\pm}}^2 |j_a^{++}|^2 + \mu_{Sj_a} S |j_a^{++}|^2 + \left[\lambda_{11}^{(a)} \Sigma_0^* h_1^- h_1^- j_a^{++} + \mu_{22}^{(a)} h_2^+ h_2^+ j_a^{--} + \text{h.c.} \right] \right\}, \end{aligned} \quad (2.9)$$

with

$$m_{j_a^{\pm\pm}}^2 \equiv \hat{m}_{j_a^{\pm\pm}}^2 + \hat{\mu}_{Sj_a} \langle S \rangle + \hat{\lambda}_{Sj_a} \langle S \rangle^2, \quad \mu_{Sk} \equiv \hat{\mu}_{Sk} + 2\hat{\lambda}_{Sk} \langle S \rangle, \quad \mu_{Sj_a} \equiv \hat{\mu}_{Sj_a} + 2\hat{\lambda}_{Sj_a} \langle S \rangle. \quad (2.10)$$

The squared physical masses of S and $j_a^{\pm\pm}$ are m_S^2 and $m_{j_a^{\pm\pm}}^2$, respectively and we set m_S as 750 GeV for our explanation of the 750 GeV excess. $j_a^{\pm\pm}$ has the same charges as $k^{\pm\pm}$ and then

can contribute to the three-loop induced neutrino masses shown in Fig. 1. The trilinear terms in the square brackets are required for evading the stability of $j_a^{\pm\pm}$. Here for brevity, we simply ignore the possible terms allowed by the symmetries, such as $|j_a^{++}|^2|\Phi|^2$, $|j_a^{++}|^2|\Sigma_0|^2$, $S|\Phi|^2$, $S|\Sigma_0|^2$ in Eq. (2.8). A large VEV of S generates large effective trilinear couplings μ_{Sk} and μ_{Sj_a} through the original terms $S^2|k^{++}|$ and $S^2|j_a^{++}|$, respectively even when the dimensionless coefficients $\hat{\lambda}_{Sk}$ and $\hat{\lambda}_{Sj_a}$ are not so large.

3 Analysis

3.1 Formulation of $p(\gamma)p(\gamma) \rightarrow S + X \rightarrow \gamma\gamma + X$

Note that under the assumption that additional interactions are only ones shown in Eq. (2.9), possible decay branches of S up to the one-loop level is to $\gamma\gamma$, $Z\gamma$, ZZ and $k^{++}k^{--}$ or $j_a^{++}j_a^{--}$. We assume that $m_{k^{\pm\pm}}$ and $m_{j_a^{\pm\pm}}$ are greater than $m_S/2$ ($= 375$ GeV), where the last two decay channels at the tree level are closed kinematically. In the present case that no tree-level decay branch is open and only $SU(2)_L$ singlet charged scalars describe the loop-induced partial widths, the relative strengths among $\Gamma_{S \rightarrow \gamma\gamma}$, $\Gamma_{S \rightarrow Z\gamma}$, $\Gamma_{S \rightarrow ZZ}$ and $\Gamma_{S \rightarrow W^+W^-}$ are governed by quantum numbers at the one-loop level¹ as

$$\Gamma_{S \rightarrow \gamma\gamma} : \Gamma_{S \rightarrow Z\gamma} : \Gamma_{S \rightarrow ZZ} : \Gamma_{S \rightarrow W^+W^-} \approx 1 : 2 \left(\frac{s_W^2}{c_W^2} \right) : \left(\frac{s_W^4}{c_W^4} \right) : 0. \quad (3.1)$$

In the following, we calculate $\Gamma_{S \rightarrow ZZ}$ in a simplified way of $\Gamma_{S \rightarrow ZZ} \approx s_W^2/(2c_W^2)\Gamma_{S \rightarrow Z\gamma} \simeq 0.15 \Gamma_{S \rightarrow Z\gamma}$.

Here, we represent a major part of partial decay widths of S with our notation for loop functions with the help of Refs. [169–173]. In the following part, for simplicity, we set all the masses of the doubly charged scalars $m_{j_a^{\pm\pm}}$ as the same as $m_{k^{\pm\pm}}$, while we ignore the contributions from the two singly charged scalars $h_{1,2}^\pm$ since they should be heavy as at least around 3 TeV and decoupled as mentioned in Appendix. The concrete form of $\Gamma_{S \rightarrow \gamma\gamma}$ and $\Gamma_{S \rightarrow Z\gamma}$ are given as

$$\Gamma_{S \rightarrow \gamma\gamma} = \frac{\alpha_{\text{EM}}^2 m_S^3}{256\pi^3} \left| \frac{1}{2} \frac{v}{m_{k^{\pm\pm}}^2} Q_k^2 C_{Skk} A_0^{\gamma\gamma}(\tau_k) \right|^2, \quad (3.2)$$

$$\Gamma_{S \rightarrow Z\gamma} = \frac{\alpha_{\text{EM}}^2 m_S^3}{512\pi^3} \left(1 - \frac{m_Z^2}{m_S^2} \right)^3 \left| -\frac{v}{m_{k^{\pm\pm}}^2} (2Q_k g_{Zkk}) C_{Skk} A_0^{Z\gamma}(\tau_k, \lambda_k) \right|^2, \quad (3.3)$$

with

$$C_{Skk} = \left(\frac{1}{v} \right) \left[\mu_{Sk} + \sum_{a=1}^{N_j} \mu_{Sj_a} \right], \quad g_{Zkk} = -Q_k \left(\frac{s_W}{c_W} \right), \quad \tau_k = \frac{4m_{k^{\pm\pm}}^2}{m_S^2}, \quad \lambda_k = \frac{4m_{k^{\pm\pm}}^2}{m_Z^2}. \quad (3.4)$$

Q_k ($= 2$) is the electric charge of the doubly charged scalars in unit of the positron's one. c_W and s_W are the cosine and the sine of the Weinberg angle θ_W , respectively. α_{EM} is the electromagnetic fine structure constant. In the following calculation, we use $s_W^2 = 0.23120$ and $\alpha_{\text{EM}} = 1/127.916$. The loop factors take the following forms,

$$A_0^{\gamma\gamma}(x) = -x^2 [x^{-1} - f(x^{-1})],$$

$$A_0^{Z\gamma}(x, y) = \frac{xy}{2(x-y)} + \frac{x^2 y^2}{2(x-y)^2} [f(x^{-1}) - f(y^{-1})] + \frac{x^2 y}{(x-y)^2} [g(x^{-1}) - g(y^{-1})], \quad (3.5)$$

¹The branching fractions are easily understood in an effective theory with the standard model gauge symmetries. See e.g. [168] with $s_2 = 0$ in the paper.

The two functions $f(z)$ and $g(z)$ ($z \equiv x^{-1}$ or y^{-1}) are formulated as

$$f(z) = \arcsin^2 \sqrt{z} \quad \text{for } z \leq 1, \quad (3.6)$$

$$g(z) = \sqrt{z^{-1} - 1} \arcsin \sqrt{z} \quad \text{for } z \leq 1, \quad (3.7)$$

where the situation $m_S \leq 2m_{k\pm\pm}$, $m_Z \leq 2m_{k\pm\pm}$ corresponds to $z \leq 1$. For simplicity, we assume the relation

$$\mu_{Sk} = \mu_{Sja}, \quad (3.8)$$

for all a .

For the production of S corresponding to the 750 GeV resonance, we consider the photon fusion process, as recently discussed in Refs. [32, 38]. In the following part, the general formulation discussed in Ref. [38] is introduced. The resonant parton-level cross section of the process $A+B \rightarrow S \rightarrow C+D$ is generally formulated as

$$\hat{\sigma}(\hat{s}) = 32\pi \frac{2J_S + 1}{(2J_A + 1)(2J_B + 1)} \frac{\Gamma_{AB}\Gamma_{CD}}{(\hat{s} - m_S^2)^2 + m_S^2\Gamma_S^2}, \quad (3.9)$$

where the factors $(2J+1)$ show spin multiplicities of the initial and the resonant states. The factor takes 2 (1) for the initial photons (the scalar resonance), respectively. By adopting the narrow width approximation (NWA) and effective photon approximation, the cross section is given with the convolution with the photon parton distribution function (PDF) $f_s^\gamma(x)$ at $s = E_{\text{CM}}^2$ as

$$\begin{aligned} \sigma(p(\gamma)p(\gamma) \rightarrow S + X \rightarrow \gamma\gamma + X) &= \int dx_1 dx_2 f_s^\gamma(x_1) f_s^\gamma(x_2) \hat{\sigma}(x_1 x_2 s) \\ &= \frac{8\pi^2 \Gamma_S}{s m_S} \mathcal{B}^2(S \rightarrow \gamma\gamma) (2J_S + 1) \int_{x_{\min}}^{x_{\max}} \frac{dx}{x} f_s^\gamma(x) f_s^\gamma\left(\frac{m_S^2}{xs}\right), \end{aligned} \quad (3.10)$$

with the two parton fractions $x_{1,2}$ with $\hat{s} = x_1 x_2 s$ at the first line. At the second line, we integrated the delta function originating from NWA. x_{\min} and x_{\max} represent the lower and upper values of the range of the integral.

Besides, we adopt the equivalent photon (or Weizsacker–Williams) approximation [174, 175] which gives the dominant contribution to the photon PDF in the diphoton production process for small x as [176, 177]

$$f_s^\gamma(x) = \frac{1}{x} \frac{2\alpha_{\text{EW}}}{\pi} \log \left[\frac{q_*}{m_p} \frac{1}{x} \right], \quad (3.11)$$

where $m_p (= 938.272 \text{ MeV})$ is the proton mass [178], and $q_* \sim \mathcal{O}(100) \text{ MeV}$ shows the inverse of the minimum impact parameter for elastic scattering, naively it being the radius of the proton. We take $q_* = (130 - 170) \text{ MeV}$ in our numerical analysis below. Now, we can exactly execute the integration over x and obtain the result,

$$\sigma(p(\gamma)p(\gamma) \rightarrow S + X \rightarrow \gamma\gamma + X) = \frac{128\alpha_{\text{EW}}^2 \Gamma_S}{3m_S^3} \mathcal{B}^2(S \rightarrow \gamma\gamma) (2J_S + 1) \log^3 \left[\frac{r_*}{r_m} \right], \quad (3.12)$$

with $r_* \equiv q_*/m_p$ and $r_m \equiv m_S/\sqrt{s}$. For a scalar resonance ($J_S = 0$) with $m_S = 750 \text{ GeV}$ and $q_* = (130 - 170) \text{ MeV}$, we obtain the following values

$$\sigma(pp \rightarrow S + X \rightarrow \gamma\gamma + X) = \left(\frac{\Gamma_S}{45 \text{ GeV}} \right) \times \mathcal{B}^2(S \rightarrow \gamma\gamma) \times \begin{cases} (6.5 - 31) \text{ fb} & , \sqrt{s} = 8 \text{ TeV}, \\ (73 - 162) \text{ fb} & , \sqrt{s} = 13 \text{ TeV}. \end{cases} \quad (3.13)$$

3.2 Results

Under our assumptions, the relevant parameters are $(m_{k\pm\pm}, \mu_{Sk}, N_j)$: the universal physical mass of the doubly charged scalars, the universal effective scalar trilinear coupling, and the number of the additional doubly charged singlet scalars. We observe the unique relation among the branching ratios of S irrespective of $m_{k\pm\pm}$ and μ_{Sk} , which is suggest by Eq. (3.1), as

$$\mathcal{B}(S \rightarrow \gamma\gamma) \simeq 0.591, \quad \mathcal{B}(S \rightarrow \gamma Z) \simeq 0.355, \quad \mathcal{B}(S \rightarrow ZZ) \simeq 0.0535. \quad (3.14)$$

In Fig. 2, situations in our model are summarized. The blue and red curves show the points of $\{m_{k\pm\pm}, \mu_{Sk}\}$ predicting $\Gamma_S = 45 \text{ GeV}$ and $\Gamma_S = 5.3 \text{ GeV}$, respectively. The value 45 GeV is the best-fit value of Γ_S reported from the ATLAS experiment [1], while the value 5.3 GeV is the experimental resolution $\sigma_E^{\gamma\gamma}$ used in the analysis of [14]. Six cases with different numbers of doubly charged scalars are considered with $N_j = 0, 1, 10, 100, 500$ and 1000 .

As pointed out in Eq. (3.14), the value of $\mathcal{B}(S \rightarrow \gamma\gamma)$ is uniquely fixed as $\simeq 60\%$ in the present model. From the values in Eqs. (1.1) and (1.2), we set our target cross section $\sigma(pp \rightarrow S + X \rightarrow \gamma\gamma + X)$ at the $\sqrt{s} = 13 \text{ TeV}$ LHC as $2 \sim 10 \text{ fb}$ within a 2σ confidence level from the central value $\simeq 6 \text{ fb}$. The green regions in Fig. 2 indicate the areas where we obtain the central value (6 fb) at $\sqrt{s} = 13 \text{ TeV}$ in the production cross section of $p(\gamma)p(\gamma) \rightarrow S + X \rightarrow \gamma\gamma + X$ with varying the parameter q_* from 130 MeV to 170 MeV , which is related to the two choices of the factorization scale of the photon PDF [defined in Eq. (3.11)] discussed in Ref. [38]. The upper and lower boundaries correspond to the cases of $q_* = 130 \text{ MeV}$ and $q_* = 170 \text{ MeV}$, respectively. On the other hand, the yellow regions, on which the green regions are superimposed, show the area where we obtain the 0.6 fb cross section at $\sqrt{s} = 8 \text{ TeV}$.

Also, we report that when we consider the case with $q_* = 170 \text{ MeV}$, the total width Γ_S should be within $[1.59 \text{ GeV}, 7.95 \text{ GeV}]$ to realize the cross section within $2 \sim 10 \text{ fb}$ from Eq. (3.13). On the other hand in $q_* = 130 \text{ MeV}$, the favored range of Γ_S is $[3.53 \text{ GeV}, 17.6 \text{ GeV}]$ from Eq. (3.13) if the cross section is within $2 \sim 10 \text{ fb}$. We find a tension with the ATLAS best fit value $\Gamma_S = 45 \text{ GeV}$ in our scenario, which is apparently suggested from panels in Fig. 2.² From now on, our target value in Γ_S is set as 5.3 GeV .

² When $\Gamma_S = 45 \text{ GeV}$, from Eq. (3.13), the target value of $\mathcal{B}(S \rightarrow \gamma\gamma + X)$ to realize $\sigma(p(\gamma)p(\gamma) \rightarrow S + X \rightarrow \gamma\gamma + X) = 6 \text{ fb}$ becomes 0.192 (when $q_* = 170 \text{ MeV}$) and 0.287 (when $q_* = 130 \text{ MeV}$).

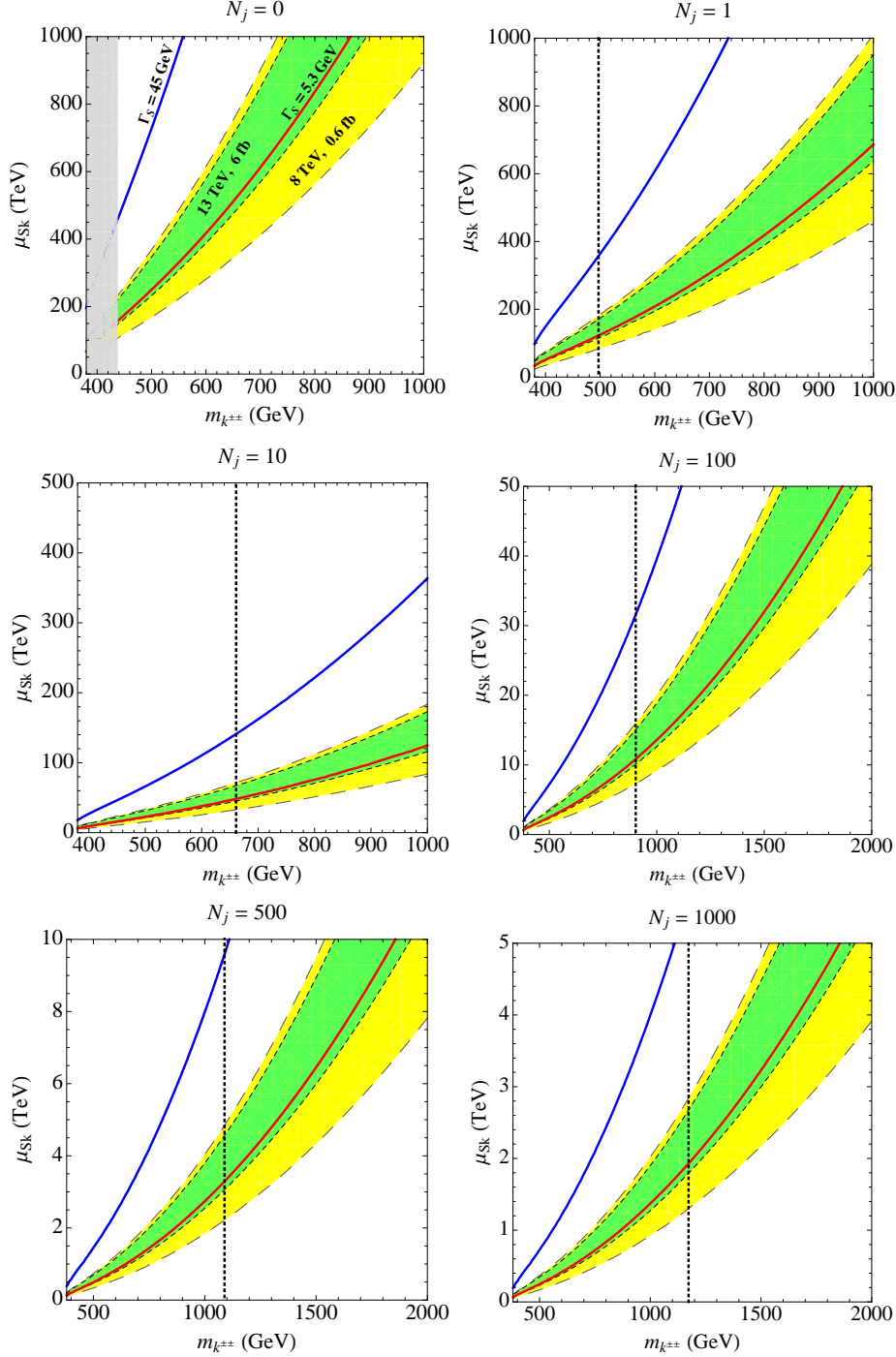


Figure 2: The blue and red curves show the points of $\{m_{k^{\pm\pm}}, \mu_{Sk}\}$ predicting $\Gamma_S = 45$ GeV and $\Gamma_S = 5.3$ GeV, respectively. Six cases with different numbers of doubly charged scalars are considered with $N_j = 0, 1, 10, 100, 500$ and 1000 . The green (yellow) regions indicate the areas where we obtain 6 fb (0.6 fb) in the production cross section of $p(\gamma)p(\gamma) \rightarrow S + X \rightarrow \gamma\gamma + X$ with varying the parameter q_* from 130 MeV (upper boundaries) to 170 MeV (lower boundaries) evaluated by Eq. (3.12). The gray shaded region $m_{k^{\pm\pm}} \leq 438$ GeV in $N_j = 0$ shows the excluded parts in 95% C.L. via the ATLAS 8 TeV data with the assumption of $\mathcal{B}(k^{\pm\pm} \rightarrow \mu^\pm \mu^\pm) = 100\%$ [179]. The vertical black dotted lines represent corresponding bounds on the universal physical mass $m_{k^{\pm\pm}}$ when we assume $\mathcal{B}(j_a^{\pm\pm} \rightarrow \mu^\pm \mu^\pm) = 100\%$ for all $j_a^{\pm\pm}$.

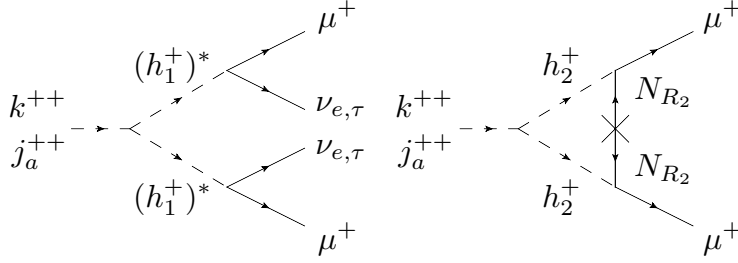


Figure 3: A schematic description for the decay patterns of k^{++} or j_a^{++} with two anti-muons in the final state. Here, h_1^+ 's in the left diagram are off-shell particles.

We comment on the bound from the 8 TeV LHC results. As mentioned in [14], the bound $\sigma(pp \rightarrow S + X \rightarrow Z\gamma + X)|_{8\text{TeV}} = 5.75 \text{ fb}$ from [180] with $\mathcal{B}(Z \rightarrow \ell\ell) = 0.06$. From Eqs. (1.3) and (1.4), we consider $\sigma(pp \rightarrow S)|_{8\text{TeV}}$ as 0.6 fb. From Eq. (3.14), we evaluate $\sigma(pp \rightarrow S + X \rightarrow Z\gamma + X)|_{8\text{TeV}} \simeq 0.21 \text{ fb}$ and conclude that the 8 TeV bound is not harmful for our case.

Here, we should mention an important issue. As indicated in Fig. 2, when N_j is zero, more than 100 TeV is required in the effective trilinear coupling μ_{Sk} . Such a large trilinear coupling immediately leads to the violation of tree level unitarity in the scattering amplitudes including μ_{Sk} , e.g., $k^{++}k^{--} \rightarrow k^{++}k^{--}$ or $SS \rightarrow k^{++}k^{--}$ at around the energy 1 TeV, where the physics with our interest is spread. Also, the vacuum is possibly threatened by the destabilization via the large trilinear coupling, which calls charge breaking minima. To evade the problems, naively speaking, the value of μ_{Sk} is less than $1 \sim 10 \text{ TeV}$.³ As shown in Fig. 2, when we introduce additional charged scalars, we can realize $\Gamma_S = 5.3 \text{ GeV}$ with a smaller value of the common effective trilinear coupling μ_{Sk} . But, we should consider the bound on the doubly charged singlet scalars from the LHC 8 TeV data. Note that the production channel of a $SU(2)_L$ singlet doubly charged scalar $k^{\pm\pm}$ is the following pair creation, $pp \rightarrow \gamma^*/Z + X \rightarrow k^{++}k^{--} + X$.

Lower bounds at 95% C.L. on $m_{k^{\pm\pm}}$ via the 8 TeV LHC data were provided by the ATLAS group in Ref. [179] as 374 GeV, 402 GeV, 438 GeV when assuming a 100% branching ratio to $e^\pm e^\pm$, $e^\pm \mu^\pm$, $\mu^\pm \mu^\pm$ pairs, respectively. In our model, the doubly charged scalars can decay through the processes as shown in Fig. 3, where h_1^+ 's are off shell since it should be heavy at least 3 TeV. In the case of k^{++} in $N_j = 0$, when the values of μ_{11} and μ_{22} are the same or similar, from Eq. (2.2), the relative branching ratios between $k^{++} \rightarrow \mu^+ \mu^+ \nu_i \nu_j$ and $k^{++} \rightarrow \mu^+ \mu^+$ are roughly proportional to $(y_L)_{2i}(y_L)_{2j}$ and $((y_R)_{22})^2$. As concluded in our previous work [146], the absolute value of $(y_R)_{22}$ should be large as around $8 \sim 9$ to generate the observed neutrino properties, while a typical magnitude of $(y_L)_{2i}$ is $0.5 \sim 1$. Then, the decay branch $k^{++} \rightarrow \mu^+ \mu^+$ is probably dominant as $\sim 100\%$ and we need to consider the 8 TeV bound seriously. A simplest attitude would be to avoid to examine the shaded regions in Fig. 2, which indicate the excluded parts in 95% C.L. via the ATLAS 8 TeV data with the assumption of $\mathcal{B}(k^{\pm\pm} \rightarrow \mu^\pm \mu^\pm) = 100\%$ [179].

When one more doubly charged scalar $j_1^{\pm\pm}$ ($N_j = 1$) exists, a detailed analysis is needed for precise bounds on $k^{\pm\pm}$ and $j_1^{\pm\pm}$. Benchmark values are given in Fig. 2 by the vertical black dotted lines, which represent corresponding bounds on the universal physical mass $m_{k^{\pm\pm}}$ when we assume $\mathcal{B}(j_a^{\pm\pm} \rightarrow \mu^\pm \mu^\pm) = 100\%$ for all $j_a^{\pm\pm}$. We obtain the 95% C.L. lower bounds on the universal mass value $m_{k^{\pm\pm}}$ as $\sim 500 \text{ GeV}$ ($N_j = 1$), $\sim 660 \text{ GeV}$ ($N_j = 10$), $\sim 900 \text{ GeV}$ ($N_j =$

³ In the case of MSSM with a light \tilde{t}_1 (100 GeV), $A = A_t = A_b$, $\tan\beta \gg 1$, $m_A \gg M_Z$, $|\mu| \ll M_{\tilde{Q}}$ and $M_{\tilde{b}}$, the bound on the trilinear coupling $|A| \lesssim 5 \text{ TeV}$ was reported in Ref. [181].

100), ~ 1090 GeV ($N_j = 500$), and ~ 1170 GeV ($N_j = 1000$), respectively through the numerical simulations by **MadGraph5** [182] with the help of **FeynRules** [183] for model implementation.

The method which we adopt for evaluating the corresponding 95% C.L. bounds with the assumption of $\mathcal{B}(j_a^{\pm\pm} \rightarrow \mu^\pm \mu^\pm) = 100\%$ for all $j_a^{\pm\pm}$, where more than one doubly charged scalars exist, is as follows. When N number of doubly charged scalars are present, the expected number of the total signal receives the multiplicative factor N . Following this statement, we can estimate the bound on the universal mass $m_{k^{\pm\pm}}$ via the pair production cross section of a doubly charged scalar $k^{\pm\pm}$ (in $N = 1$ case) though the sequence $pp \rightarrow \gamma^*/Z + X \rightarrow k^{++}k^{--} + X$. The bound should correspond to the mass where the production cross section is N -times smaller than the benchmark value in $m_{k^{\pm\pm}} = 438$ GeV, which is the 95% C.L lower bound on $m_{k^{\pm\pm}}$ from the ATLAS 8 TeV data [179]. We obtained the leading order cross section as 0.327 fb. Note that this digit is close to the ATLAS official value, 0.357 fb read from Fig. 4 (c) of Ref. [179]. In calculation, we used CTEQ6L proton PDF [184] and set the renormalization and factorization scales as $2m_{k^{\pm\pm}}$.

Here, we point out an interesting possibility. From Eq. (2.9), if $\lambda_{11}^{(1)} \langle \Sigma_0^* \rangle$ is quite larger than $\mu_{22}^{(1)}$, the pattern $j_1^{++} \rightarrow \mu^+ \mu^+ \nu_i \nu_j$ possibly becomes considerable, where we cannot reconstruct the invariant mass of the doubly charged scalar since missing energy exists in this decay sequence. Then, significance for exclusion would be dropped and we could relax the bound on $m_{j_1^{\pm\pm}}$ to some extent. An extreme case is with a nonzero $\lambda_{11}^{(1)} \langle \Sigma_0^* \rangle$ and $\mu_{22}^{(1)} = 0$, where the branching ratio of $j_1^{++} \rightarrow \mu^+ \mu^+$ becomes zero at the one loop level and the significance takes the lowest value, which is the best for evading the 8 TeV LHC bound. Also in this situation, no additional contribution to the neutrino mass matrix exists and the original successful structure is not destroyed. Similar discussions are applicable when N_j is more than one.

When we assume 100% branching fractions in $j_a^{++} \rightarrow \mu^+ \mu^+$ for all j_a^{++} , the common trilinear coupling μ_{Sk} should be larger than ~ 150 TeV ($N_j = 0$), ~ 120 TeV ($N_j = 1$), ~ 40 TeV ($N_j = 10$), ~ 10 TeV ($N_j = 100$), ~ 3 TeV ($N_j = 500$), ~ 2 TeV ($N_j = 1000$) to obtain $\Gamma_S = 5.3$ GeV and a reasonable amount of the production cross section around 6 fb as suggested by Fig. 2. As mentioned, large trilinear couplings $\lambda_{11}^{(a)} \langle \Sigma_0^* \rangle$ can help us to alleviate the 8 TeV bound.

Unfortunately when $N_j = 0$ or a few, explaining the diphoton excess is not consistent with tree level unitarity since the value of μ_{Sk} is very large and tree level unitarity is violated. There would be a hope in $N_j = 10$ if the significance can be deteriorated as the lower bound on $m_{k^{\pm\pm}}$ is dropped around the kinematic boundary $m_S/2 = 375$ GeV. In the case of $N_j = 100$, a small drop is enough in the branching ratios for explaining the 750 GeV excess consistently. If we accept the configuration $N_j = 500$ or 1000, the lower bound on μ_{Sk} would decrease as a few TeV, where tree level unitarity has no problem. In these cases, we can explain the 750 GeV excess consistently even when $\mathcal{B}(j_a^{\pm\pm} \rightarrow \mu^\pm \mu^\pm) = 100\%$ for all $j_a^{\pm\pm}$.⁴

4 Conclusion and discussion

In this paper, we investigated a possibility for explaining the recently announced 750 GeV diphoton excess by the ATLAS and the CMS experiments at the CERN LHC in the context of loop induced singlet production and decay through photon fusion. When a singlet scalar S , which is a candidate of the particle in the resonance, couples to charged particles, we can obtain a suitable amount of

⁴ The key point is as follows. When we consider N doubly charged scalars, the amplitude obtains the multiplicative factor N , which means the partial decay width receives the factor N^2 . On the other hand, all of the particles should be distinguished in the final state as $pp \rightarrow k^{++}k^{--}, j_a^{++}j_a^{--}$. Then, the expected number of signals obtain the factor N (not N^2) at the parton level. Also, an extra suppression by proton PDF is expected.

the cross section of $pp \rightarrow S + X \rightarrow \gamma\gamma + X$ without assuming a tree-level production of S . In three-loop radiative neutrino models, $SU(2)_L$ singlet multiple doubly-charged scalars are introduced such that the $S - \gamma - \gamma$ vertex is radiatively generated and enhanced. When we consider such type of doubly-charged scalar(s), the branching ratio $\mathcal{B}(S \rightarrow \gamma\gamma)$ is uniquely fixed as $\simeq 60\%$ by quantum numbers, where constraints from 8 TeV LHC data are all satisfied.

A fascinating feature in the single S production through photon fusion is that the value of $\mathcal{B}(S \rightarrow \gamma\gamma)$ as well as Γ_S determines the production cross section, as shown in Eq. (3.13). In the above $S \rightarrow \gamma\gamma$ branching fraction ($\simeq 60\%$), when $\Gamma_S = 45 \text{ GeV}$ (ATLAS best-fit value), too large cross section is predicted. On the other hand when $\Gamma_S \simeq 5.3 \text{ GeV}$ (experimental resolution), the realized cross section is close to the central value $\simeq 6 \text{ fb}$. This is an informative prediction of our present scenario and tested in the near future. Also in our configuration, the relative strengths of the one loop induced partial decay widths are fixed by quantum numbers irrespective of N_j as shown in Eq. (3.1). This universality is a remarkable property of our scenario and this relation can be tested after much amount of data is accumulated.

From the consistency with tree level unitarity, multiple additional doubly charged scalars should be introduced. This is also an interesting prediction in our scenario. The required minimum in the total number of the doubly charged particles would be located at $10 \sim 100$ (or a bit more), which depends on the significance of the channel(s), $j_a^{++} \rightarrow \mu^+ \mu^+ \nu_i \nu_j$. The situation with multiple doubly charged scalars is also very stimulating in collider physics point of view.

Finally, we discuss further extensions of the model and other phenomenological issues.

- A possible extension of the present direction is to introduce N_S number of $SU(2)_L$ singlet scalars, ($S = S_1, S_2, \dots, S_{N_S}$), without hypercharge in the theory. If the masses of the scalars are almost degenerate to 750 GeV, the current experiment may not be able to detect the multi bumps so that they would look as a single bump as we face. The total cross section, then, is enhanced by the multiplicative factor of N_S^2 as

$$\sigma_{\text{tot}}(pp \rightarrow \gamma\gamma + X) \approx N_S^2 \sigma(pp \rightarrow S + X \rightarrow \gamma\gamma + X). \quad (4.1)$$

- Another possible extension is that we also introduce the singly charged scalars $\tilde{h}_{1,2}^\pm$ which hold the same quantum numbers as $h_{1,2}^\pm$ and has the same interaction with $j_a^{\pm\pm}$ as $h_{1,2}^\pm$ do with $k^{\pm\pm}$. In such a possibility, contributions to the neutrino mass matrix are enhanced and we can reduce the value of the large coupling required for a consistent explanation in the original model, especially in $(y_R)_{22}$. See Appendix for details.
- The triple coupling of the Higgs boson could be enhanced in our case that may activate the strong first order phase transition, which is a necessity for realizing the electroweak baryogenesis scenario [185]. In such a case, radiative seesaw models can explain not only neutrino mass and dark matter but also baryon asymmetry of the Universe.
- The decays $k^{\pm\pm} \rightarrow \ell^\pm \ell^\pm$ and $j_a^{\pm\pm} \rightarrow \ell^\pm \ell^\pm$ provide very clean signatures. The 13 TeV LHC would be expected to replace the current bound on the universal mass, e.g., $m_{k^{\pm\pm}} > 438 \text{ GeV}$ when $\mathcal{B}(k^\pm/j_a^\pm \rightarrow \mu^\pm \mu^\pm) = 100\%$ for all the doubly charged scalars, from the 8 TeV data [179] soon. An important feature recognized from Fig. 2 is that when N_j is not so large as around $10 \sim 100$, only light doubly charged scalars are consistent with the bound from tree level unitarity. Such possibilities would be exhaustively surveyed and eventually confirmed or excluded in the near future. On the other hand, when N_j is large as around $500 \sim 1000$, from Fig. 2, more than 1 TeV doubly charged scalars can exist with holding tree level unitarity.

Such heavy particles require a suitable amount of integrated luminosity for being tested in colliders. In other words, such possibilities are hard to be discarded in the near future.

- It might be worth mentioning the discrimination between our model discussed here and the other well known radiative models, namely, Zee model [127] at the one-loop level, Zee-Babu model [129, 130] at the two-loop level, Kraus-Nasri-Trodden (KNT) model [132], Aoki-Kanemura-Seto (AKS) model [133, 134], and Gustafsson-No-Rivera (GNR) model [135] at the three-loop level. Essentially, any model that includes isospin singlet charged bosons potentially explain the 750 GeV diphoton excess along the same way as discussed in this paper. Among those, three-loop models have natural DM candidates by construction, which we regard as a phenomenological big advantage. Our model shares this virtue. On the other hand, in view of the charged-boson, our model and also the GNR model include doubly charged particles. From the currently available data, it is not possible to distinguish the effect of a singly charged scalar from a double charged scalar. However, we still see that a doubly charged boson is in favor of the explanation of the 750 GeV diphoton excess simply because of the enhanced diphoton coupling.
- As we discussed before, $k^{\pm\pm}$ decays to $\mu^\pm\mu^\pm$ with an almost 100% branching fraction, distinctively from other models, e.g., Zee-Babu model, due to the large coupling $(y_R)_{22} \gtrsim 2\pi$, which is required to realize the observed neutrino data in our setup consistently.

Acknowledgements

SK, KN, YO, and SCP thank the workshop, Yangpyung School 2015, for providing us an opportunity to initiate this collaboration. We are grateful for Eung Jin Chun, Satoshi Iso, Takaaki Nomura and Hiroshi Yokoya for fruitful discussions. SK was supported in part by Grant-in-Aid for Scientific Research, The Ministry of Education, Culture, Sports, Science and Technology (MEXT), No. 23104006, and Grant H2020-MSCA-RISE- 2014 No. 645722 (Non-Minimal Higgs). This work is supported in part by NRF Research No. 2009-0083526 (YO) of the Republic of Korea. SCP is supported by the Basic Science Research Program through the National Research Foundation of Korea (NRF) funded by the Ministry of Education, Science and Technology based on contract number 2013R1A1A2064120. This work was supported by IBS under the project code, IBS-R018-D1 for RW.

Appendix

Here, we briefly summarize features in the model discussed in [146].

- (a) In this model, the sub-eV neutrino masses are radiatively generated at the three loop level with the loop suppression factor $1/(4\pi)^6$. In such a situation, a part of couplings, including scalar trilinear couplings, contributing to the neutrino matrix tends to be close to unity.
- (b) When a scalar trilinear coupling is large, they can put a negative effect on scalar quartic couplings at the one loop level, which threatens the stability of the vacuum.
- (c) The doubly charged scalar $k^{\pm\pm}$ is isolated from the charged lepton at the leading order under the assignment of the global $U(1)$ charges summarized in Tab. 1. Then, the charged particle

does not contribute to lepton-flavor-violating processes significantly and a few hundred GeV mass is possible.

- (d) The two singly charged scalars h_1^\pm and h_2^\pm have couplings to the charged leptons at the tree level. Since in our model a part of couplings are sizable, constraints from lepton flavor violations and vacuum stability do not allow a few hundred GeV masses, especially when $k^{\pm\pm}$ is around a few hundred GeV. The result of the global analysis in our previous paper [146] says that when $k^{\pm\pm}$ is 250 GeV (which is around the minimum value of $m_{k^{\pm\pm}}$), $m_{h_1^\pm}$ and $m_{h_2^\pm}$ should be greater than 3 TeV.
- (e) In allowed parameter configurations, we found that the absolute value of the coupling $(y_R)_{22}$ (in front of $\bar{N}_{R2} e_{R2}^c h_2^-$), tends to be $8 \sim 9$, while the peak of the distribution of the scalar trilinear couplings $\mu_{11} \equiv \lambda_{11} v' / \sqrt{2}$ (in front of $h_1^- h_1^- k^{++}$) and μ_{22} (in front of $h_2^+ h_2^+ k^{--}$) is around $14 \sim 15$ TeV. Note that we assumed that values of μ_{11} and μ_{22} are the same and real in the analysis.
- (f) The two CP even components are mixed each other as shown in Eq. (2.4). By the (simplified) global analysis in [146] based on the data [186–191], the sine of the mixing angle α should be

$$|\sin \alpha| \lesssim 0.3, \quad (4.2)$$

within 2σ allowed regions.

- (g) On the other hand, the observed relic density requires a specific range of $\sin \alpha$. In our model, the Majorana DM N_{R1} communicates with the SM particles and the $U(1)$ NG boson G through the two CP even scalars h and H . When v' is $\mathcal{O}(1)$ TeV, DM–DM– h/H couplings are significantly suppressed as (M_{N1}/v') and then we should rely on the two scalar resonant regions. When we consider the situation $m_{\text{DM}}/2 \simeq m_h (\simeq 125 \text{ GeV})$, a reasonable amount of the mixing angle α is required as

$$|\sin \alpha| \gtrsim 0.3, \quad (4.3)$$

where a tense situation with Eq. (4.2) is observed. The allowed range of v' is a function of $\sin \alpha$ and the maximum value is

$$v'|_{\text{max}} \sim 9 \text{ TeV when } |\sin \alpha| \sim 0.3. \quad (4.4)$$

Whereas the other resonant point is selected as $m_{\text{DM}}/2 \simeq m_H$, the requirement on the angle is as follows,

$$|\sin \alpha| \lesssim 0.3, \quad (4.5)$$

when $m_H = 250 \text{ GeV}$ or a bit more. We find that the heavy H as $m_H = 500 \text{ GeV}$ cannot explain the relic density because of the suppression in the resonant propagator of H . The maximum of v' is found as

$$v'|_{\text{max}} \sim 6 \text{ TeV when } 0 \lesssim |\sin \alpha| \lesssim 0.05, \quad (4.6)$$

where the couplings of H to the SM particles becomes so weak and hard to be excluded from the 8 TeV LHC results.

References

- [1] “Search for resonances decaying to photon pairs in 3.2 fb^{-1} of pp collisions at $\sqrt{s} = 13 \text{ TeV}$ with the ATLAS detector,” Tech. Rep. ATLAS-CONF-2015-081, CERN, Geneva, Dec, 2015.
- [2] CMS Collaboration, “Search for new physics in high mass diphoton events in proton-proton collisions at $\sqrt{s} = 13 \text{ TeV}$,” Tech. Rep. CMS-PAS-EXO-15-004, CERN, Geneva, 2015.
- [3] K. Harigaya and Y. Nomura, “Composite Models for the 750 GeV Diphoton Excess,” [arXiv:1512.04850 \[hep-ph\]](#).
- [4] Y. Mambrini, G. Arcadi, and A. Djouadi, “The LHC diphoton resonance and dark matter,” [arXiv:1512.04913 \[hep-ph\]](#).
- [5] M. Backovic, A. Mariotti, and D. Redigolo, “Di-photon excess illuminates Dark Matter,” [arXiv:1512.04917 \[hep-ph\]](#).
- [6] A. Angelescu, A. Djouadi, and G. Moreau, “Scenarii for interpretations of the LHC diphoton excess: two Higgs doublets and vector-like quarks and leptons,” [arXiv:1512.04921 \[hep-ph\]](#).
- [7] Y. Nakai, R. Sato, and K. Tobioka, “Footprints of New Strong Dynamics via Anomaly,” [arXiv:1512.04924 \[hep-ph\]](#).
- [8] S. Knapen, T. Melia, M. Papucci, and K. Zurek, “Rays of light from the LHC,” [arXiv:1512.04928 \[hep-ph\]](#).
- [9] D. Buttazzo, A. Greljo, and D. Marzocca, “Knocking on New Physics’ door with a Scalar Resonance,” [arXiv:1512.04929 \[hep-ph\]](#).
- [10] A. Pilaftsis, “Diphoton Signatures from Heavy Axion Decays at LHC,” [arXiv:1512.04931 \[hep-ph\]](#).
- [11] R. Franceschini, G. F. Giudice, J. F. Kamenik, M. McCullough, A. Pomarol, R. Rattazzi, M. Redi, F. Riva, A. Strumia, and R. Torre, “What is the gamma gamma resonance at 750 GeV?,” [arXiv:1512.04933 \[hep-ph\]](#).
- [12] S. Di Chiara, L. Marzola, and M. Raidal, “First interpretation of the 750 GeV di-photon resonance at the LHC,” [arXiv:1512.04939 \[hep-ph\]](#).
- [13] T. Higaki, K. S. Jeong, N. Kitajima, and F. Takahashi, “The QCD Axion from Aligned Axions and Diphoton Excess,” [arXiv:1512.05295 \[hep-ph\]](#).
- [14] S. D. McDermott, P. Meade, and H. Ramani, “Singlet Scalar Resonances and the Diphoton Excess,” [arXiv:1512.05326 \[hep-ph\]](#).
- [15] J. Ellis, S. A. R. Ellis, J. Quevillon, V. Sanz, and T. You, “On the Interpretation of a Possible $\sim 750 \text{ GeV}$ Particle Decaying into $\gamma\gamma$,” [arXiv:1512.05327 \[hep-ph\]](#).
- [16] M. Low, A. Tesi, and L.-T. Wang, “A pseudoscalar decaying to photon pairs in the early LHC run 2 data,” [arXiv:1512.05328 \[hep-ph\]](#).
- [17] B. Bellazzini, R. Franceschini, F. Sala, and J. Serra, “Goldstones in Diphotons,” [arXiv:1512.05330 \[hep-ph\]](#).
- [18] R. S. Gupta, S. Jager, Y. Kats, G. Perez, and E. Stamou, “Interpreting a 750 GeV Diphoton Resonance,” [arXiv:1512.05332 \[hep-ph\]](#).
- [19] C. Petersson and R. Torre, “The 750 GeV diphoton excess from the goldstino superpartner,” [arXiv:1512.05333 \[hep-ph\]](#).
- [20] E. Molinaro, F. Sannino, and N. Vignaroli, “Strong dynamics or axion origin of the diphoton excess,” [arXiv:1512.05334 \[hep-ph\]](#).

- [21] A. Falkowski, O. Slone, and T. Volansky, “Phenomenology of a 750 GeV Singlet,” [arXiv:1512.05777 \[hep-ph\]](#).
- [22] B. Dutta, Y. Gao, T. Ghosh, I. Gogoladze, and T. Li, “Interpretation of the diphoton excess at CMS and ATLAS,” [arXiv:1512.05439 \[hep-ph\]](#).
- [23] Q.-H. Cao, Y. Liu, K.-P. Xie, B. Yan, and D.-M. Zhang, “A Boost Test of Anomalous Diphoton Resonance at the LHC,” [arXiv:1512.05542 \[hep-ph\]](#).
- [24] S. Matsuzaki and K. Yamawaki, “750 GeV Diphoton Signal from One-Family Walking Technipion,” [arXiv:1512.05564 \[hep-ph\]](#).
- [25] A. Kobakhidze, F. Wang, L. Wu, J. M. Yang, and M. Zhang, “LHC diphoton excess explained as a heavy scalar in top-seesaw model,” [arXiv:1512.05585 \[hep-ph\]](#).
- [26] R. Martinez, F. Ochoa, and C. F. Sierra, “Diphoton decay for a 750 GeV scalar dark matter,” [arXiv:1512.05617 \[hep-ph\]](#).
- [27] P. Cox, A. D. Medina, T. S. Ray, and A. Spray, “Diphoton Excess at 750 GeV from a Radion in the Bulk-Higgs Scenario,” [arXiv:1512.05618 \[hep-ph\]](#).
- [28] D. Becirevic, E. Bertuzzo, O. Sumensari, and R. Z. Funchal, “Can the new resonance at LHC be a CP-Odd Higgs boson?,” [arXiv:1512.05623 \[hep-ph\]](#).
- [29] J. M. No, V. Sanz, and J. Setford, “See-Saw Composite Higgses at the LHC: Linking Naturalness to the 750 GeV Di-Photon Resonance,” [arXiv:1512.05700 \[hep-ph\]](#).
- [30] S. V. Demidov and D. S. Gorbunov, “On sgoldstino interpretation of the diphoton excess,” [arXiv:1512.05723 \[hep-ph\]](#).
- [31] W. Chao, R. Huo, and J.-H. Yu, “The Minimal Scalar-Stealth Top Interpretation of the Diphoton Excess,” [arXiv:1512.05738 \[hep-ph\]](#).
- [32] S. Fichet, G. von Gersdorff, and C. Royon, “Scattering Light by Light at 750 GeV at the LHC,” [arXiv:1512.05751 \[hep-ph\]](#).
- [33] D. Curtin and C. B. Verhaaren, “Quirky Explanations for the Diphoton Excess,” [arXiv:1512.05753 \[hep-ph\]](#).
- [34] L. Bian, N. Chen, D. Liu, and J. Shu, “A hidden confining world on the 750 GeV diphoton excess,” [arXiv:1512.05759 \[hep-ph\]](#).
- [35] J. Chakraborty, A. Choudhury, P. Ghosh, S. Mondal, and T. Srivastava, “Di-photon resonance around 750 GeV: shedding light on the theory underneath,” [arXiv:1512.05767 \[hep-ph\]](#).
- [36] A. Ahmed, B. M. Dillon, B. Grzadkowski, J. F. Gunion, and Y. Jiang, “Higgs-radion interpretation of 750 GeV di-photon excess at the LHC,” [arXiv:1512.05771 \[hep-ph\]](#).
- [37] P. Agrawal, J. Fan, B. Heidenreich, M. Reece, and M. Strassler, “Experimental Considerations Motivated by the Diphoton Excess at the LHC,” [arXiv:1512.05775 \[hep-ph\]](#).
- [38] C. Csaki, J. Hubisz, and J. Terning, “The Minimal Model of a Diphoton Resonance: Production without Gluon Couplings,” [arXiv:1512.05776 \[hep-ph\]](#).
- [39] D. Aloni, K. Blum, A. Dery, A. Efrati, and Y. Nir, “On a possible large width 750 GeV diphoton resonance at ATLAS and CMS,” [arXiv:1512.05778 \[hep-ph\]](#).
- [40] Y. Bai, J. Berger, and R. Lu, “A 750 GeV Dark Pion: Cousin of a Dark G-parity-odd WIMP,” [arXiv:1512.05779 \[hep-ph\]](#).
- [41] E. Gabrielli, K. Kannike, B. Mele, M. Raidal, C. Spethmann, and H. Veermae, “A SUSY Inspired Simplified Model for the 750 GeV Diphoton Excess,” [arXiv:1512.05961 \[hep-ph\]](#).

- [42] R. Benbrik, C.-H. Chen, and T. Nomura, “Higgs singlet as a diphoton resonance in a vector-like quark model,” [arXiv:1512.06028 \[hep-ph\]](#).
- [43] J. S. Kim, J. Reuter, K. Rolbiecki, and R. R. de Austri, “A resonance without resonance: scrutinizing the diphoton excess at 750 GeV,” [arXiv:1512.06083 \[hep-ph\]](#).
- [44] A. Alves, A. G. Dias, and K. Sinha, “The 750 GeV S -cion: Where else should we look for it?,” [arXiv:1512.06091 \[hep-ph\]](#).
- [45] E. Megias, O. Pujolas, and M. Quiros, “On dilatons and the LHC diphoton excess,” [arXiv:1512.06106 \[hep-ph\]](#).
- [46] L. M. Carpenter, R. Colburn, and J. Goodman, “Supersoft SUSY Models and the 750 GeV Diphoton Excess, Beyond Effective Operators,” [arXiv:1512.06107 \[hep-ph\]](#).
- [47] J. Bernon and C. Smith, “Could the width of the diphoton anomaly signal a three-body decay?,” [arXiv:1512.06113 \[hep-ph\]](#).
- [48] W. Chao, “Symmetries Behind the 750 GeV Diphoton Excess,” [arXiv:1512.06297 \[hep-ph\]](#).
- [49] M. T. Arun and P. Saha, “Gravitons in multiply warped scenarios - at 750 GeV and beyond,” [arXiv:1512.06335 \[hep-ph\]](#).
- [50] C. Han, H. M. Lee, M. Park, and V. Sanz, “The diphoton resonance as a gravity mediator of dark matter,” [arXiv:1512.06376 \[hep-ph\]](#).
- [51] S. Chang, “A Simple $U(1)$ Gauge Theory Explanation of the Diphoton Excess,” [arXiv:1512.06426 \[hep-ph\]](#).
- [52] I. Chakraborty and A. Kundu, “Diphoton excess at 750 GeV: Singlet scalars confront naturalness,” [arXiv:1512.06508 \[hep-ph\]](#).
- [53] R. Ding, L. Huang, T. Li, and B. Zhu, “Interpreting 750 GeV Diphoton Excess with R-parity Violation Supersymmetry,” [arXiv:1512.06560 \[hep-ph\]](#).
- [54] H. Han, S. Wang, and S. Zheng, “Scalar Dark Matter Explanation of Diphoton Excess at LHC,” [arXiv:1512.06562 \[hep-ph\]](#).
- [55] X.-F. Han and L. Wang, “Implication of the 750 GeV diphoton resonance on two-Higgs-doublet model and its extensions with Higgs field,” [arXiv:1512.06587 \[hep-ph\]](#).
- [56] M.-x. Luo, K. Wang, T. Xu, L. Zhang, and G. Zhu, “Squarkonium/Diquarkonium and the Di-photon Excess,” [arXiv:1512.06670 \[hep-ph\]](#).
- [57] J. Chang, K. Cheung, and C.-T. Lu, “Interpreting the 750 GeV Di-photon Resonance using photon-jets in Hidden-Valley-like models,” [arXiv:1512.06671 \[hep-ph\]](#).
- [58] D. Bardhan, D. Bhatia, A. Chakraborty, U. Maitra, S. Raychaudhuri, and T. Samui, “Radion Candidate for the LHC Diphoton Resonance,” [arXiv:1512.06674 \[hep-ph\]](#).
- [59] T.-F. Feng, X.-Q. Li, H.-B. Zhang, and S.-M. Zhao, “The LHC 750 GeV diphoton excess in supersymmetry with gauged baryon and lepton numbers,” [arXiv:1512.06696 \[hep-ph\]](#).
- [60] O. Antipin, M. Mojaza, and F. Sannino, “A natural Coleman-Weinberg theory explains the diphoton excess,” [arXiv:1512.06708 \[hep-ph\]](#).
- [61] F. Wang, L. Wu, J. M. Yang, and M. Zhang, “750 GeV Diphoton Resonance, 125 GeV Higgs and Muon $g-2$ Anomaly in Deflected Anomaly Mediation SUSY Breaking Scenario,” [arXiv:1512.06715 \[hep-ph\]](#).
- [62] J. Cao, C. Han, L. Shang, W. Su, J. M. Yang, and Y. Zhang, “Interpreting the 750 GeV diphoton excess by the singlet extension of the Manohar-Wise Model,” [arXiv:1512.06728 \[hep-ph\]](#).

- [63] F. P. Huang, C. S. Li, Z. L. Liu, and Y. Wang, “750 GeV Diphoton Excess from Cascade Decay,” [arXiv:1512.06732 \[hep-ph\]](#).
- [64] W. Liao and H.-q. Zheng, “Scalar resonance at 750 GeV as composite of heavy vector-like fermions,” [arXiv:1512.06741 \[hep-ph\]](#).
- [65] J. J. Heckman, “750 GeV Diphotons from a D3-brane,” [arXiv:1512.06773 \[hep-ph\]](#).
- [66] M. Dhuria and G. Goswami, “Perturbativity, vacuum stability and inflation in the light of 750 GeV diphoton excess,” [arXiv:1512.06782 \[hep-ph\]](#).
- [67] X.-J. Bi, Q.-F. Xiang, P.-F. Yin, and Z.-H. Yu, “The 750 GeV diphoton excess at the LHC and dark matter constraints,” [arXiv:1512.06787 \[hep-ph\]](#).
- [68] J. S. Kim, K. Rolbiecki, and R. R. de Austri, “Model-independent combination of diphoton constraints at 750 GeV,” [arXiv:1512.06797 \[hep-ph\]](#).
- [69] L. Berthier, J. M. Cline, W. Shepherd, and M. Trott, “Effective interpretations of a diphoton excess,” [arXiv:1512.06799 \[hep-ph\]](#).
- [70] W. S. Cho, D. Kim, K. Kong, S. H. Lim, K. T. Matchev, J.-C. Park, and M. Park, “The 750 GeV Diphoton Excess May Not Imply a 750 GeV Resonance,” [arXiv:1512.06824 \[hep-ph\]](#).
- [71] J. M. Cline and Z. Liu, “LHC diphotons from electroweakly pair-produced composite pseudoscalars,” [arXiv:1512.06827 \[hep-ph\]](#).
- [72] M. Bauer and M. Neubert, “Flavor Anomalies, the Diphoton Excess and a Dark Matter Candidate,” [arXiv:1512.06828 \[hep-ph\]](#).
- [73] M. Chala, M. Duerr, F. Kahlhoefer, and K. Schmidt-Hoberg, “Tricking Landau-Yang: How to obtain the diphoton excess from a vector resonance,” [arXiv:1512.06833 \[hep-ph\]](#).
- [74] D. Barducci, A. Goudelis, S. Kulkarni, and D. Sengupta, “One jet to rule them all: monojet constraints and invisible decays of a 750 GeV diphoton resonance,” [arXiv:1512.06842 \[hep-ph\]](#).
- [75] G. M. Pelaggi, A. Strumia, and E. Vigiani, “Trinification can explain the di-photon and di-boson LHC anomalies,” [arXiv:1512.07225 \[hep-ph\]](#).
- [76] S. M. Boucenna, S. Morisi, and A. Vicente, “The LHC diphoton resonance from gauge symmetry,” [arXiv:1512.06878 \[hep-ph\]](#).
- [77] C. W. Murphy, “Vector Leptoquarks and the 750 GeV Diphoton Resonance at the LHC,” [arXiv:1512.06976 \[hep-ph\]](#).
- [78] A. E. C. Hernández and I. Nisandzic, “LHC diphoton 750 GeV resonance as an indication of $SU(3)_c \times SU(3)_L \times U(1)_X$ gauge symmetry,” [arXiv:1512.07165 \[hep-ph\]](#).
- [79] U. K. Dey, S. Mohanty, and G. Tomar, “750 GeV resonance in the Dark Left-Right Model,” [arXiv:1512.07212 \[hep-ph\]](#).
- [80] J. de Blas, J. Santiago, and R. Vega-Morales, “New vector bosons and the diphoton excess,” [arXiv:1512.07229 \[hep-ph\]](#).
- [81] A. Belyaev, G. Cacciapaglia, H. Cai, T. Flacke, A. Parolini, and H. Serôdio, “Singlets in Composite Higgs Models in light of the LHC di-photon searches,” [arXiv:1512.07242 \[hep-ph\]](#).
- [82] P. S. B. Dev and D. Teresi, “Asymmetric Dark Matter in the Sun and the Diphoton Excess at the LHC,” [arXiv:1512.07243 \[hep-ph\]](#).
- [83] W.-C. Huang, Y.-L. S. Tsai, and T.-C. Yuan, “Gauged Two Higgs Doublet Model confronts the LHC 750 GeV di-photon anomaly,” [arXiv:1512.07268 \[hep-ph\]](#).
- [84] S. Moretti and K. Yagyu, “The 750 GeV diphoton excess and its explanation in 2-Higgs

- Doublet Models with a real inert scalar multiplet,” [arXiv:1512.07462 \[hep-ph\]](#).
- [85] K. M. Patel and P. Sharma, “Interpreting 750 GeV diphoton excess in SU(5) grand unified theory,” [arXiv:1512.07468 \[hep-ph\]](#).
 - [86] M. Badziak, “Interpreting the 750 GeV diphoton excess in minimal extensions of Two-Higgs-Doublet models,” [arXiv:1512.07497 \[hep-ph\]](#).
 - [87] S. Chakraborty, A. Chakraborty, and S. Raychaudhuri, “Diphoton resonance at 750 GeV in the broken MRSSM,” [arXiv:1512.07527 \[hep-ph\]](#).
 - [88] Q.-H. Cao, S.-L. Chen, and P.-H. Gu, “Strong CP Problem, Neutrino Masses and the 750 GeV Diphoton Resonance,” [arXiv:1512.07541 \[hep-ph\]](#).
 - [89] W. Altmannshofer, J. Galloway, S. Gori, A. L. Kagan, A. Martin, and J. Zupan, “On the 750 GeV di-photon excess,” [arXiv:1512.07616 \[hep-ph\]](#).
 - [90] M. Cvetič, J. Halverson, and P. Langacker, “String Consistency, Heavy Exotics, and the 750 GeV Diphoton Excess at the LHC,” [arXiv:1512.07622 \[hep-ph\]](#).
 - [91] J. Gu and Z. Liu, “Running after Diphoton,” [arXiv:1512.07624 \[hep-ph\]](#).
 - [92] B. C. Allanach, P. S. B. Dev, S. A. Renner, and K. Sakurai, “Di-photon Excess Explained by a Resonant Sneutrino in R-parity Violating Supersymmetry,” [arXiv:1512.07645 \[hep-ph\]](#).
 - [93] H. Davoudiasl and C. Zhang, “A 750 GeV Messenger of Dark Conformal Symmetry Breaking,” [arXiv:1512.07672 \[hep-ph\]](#).
 - [94] N. Craig, P. Draper, C. Kilic, and S. Thomas, “How the $\gamma\gamma$ Resonance Stole Christmas,” [arXiv:1512.07733 \[hep-ph\]](#).
 - [95] K. Das and S. K. Rai, “The 750 GeV Diphoton excess in a $U(1)$ hidden symmetry model,” [arXiv:1512.07789 \[hep-ph\]](#).
 - [96] K. Cheung, P. Ko, J. S. Lee, J. Park, and P.-Y. Tseng, “A Higgcision study on the 750 GeV Di-photon Resonance and 125 GeV SM Higgs boson with the Higgs-Singlet Mixing,” [arXiv:1512.07853 \[hep-ph\]](#).
 - [97] J. Liu, X.-P. Wang, and W. Xue, “LHC diphoton excess from colorful resonances,” [arXiv:1512.07885 \[hep-ph\]](#).
 - [98] J. Zhang and S. Zhou, “Electroweak Vacuum Stability and Diphoton Excess at 750 GeV,” [arXiv:1512.07889 \[hep-ph\]](#).
 - [99] J. A. Casas, J. R. Espinosa, and J. M. Moreno, “The 750 GeV Diphoton Excess as a First Light on Supersymmetry Breaking,” [arXiv:1512.07895 \[hep-ph\]](#).
 - [100] L. J. Hall, K. Harigaya, and Y. Nomura, “750 GeV Diphotons: Implications for Supersymmetric Unification,” [arXiv:1512.07904 \[hep-ph\]](#).
 - [101] H. Han, S. Wang, and S. Zheng, “Dark Matter Theories in the Light of Diphoton Excess,” [arXiv:1512.07992 \[hep-ph\]](#).
 - [102] J.-C. Park and S. C. Park, “Indirect signature of dark matter with the diphoton resonance at 750 GeV,” [arXiv:1512.08117 \[hep-ph\]](#).
 - [103] A. Salvio and A. Mazumdar, “Higgs Stability and the 750 GeV Diphoton Excess,” [arXiv:1512.08184 \[hep-ph\]](#).
 - [104] D. Chway, R. Dermíšek, T. H. Jung, and H. D. Kim, “Glue to light signal of a new particle,” [arXiv:1512.08221 \[hep-ph\]](#).
 - [105] G. Li, Y.-n. Mao, Y.-L. Tang, C. Zhang, Y. Zhou, and S.-h. Zhu, “A Loop-philic Pseudoscalar,” [arXiv:1512.08255 \[hep-ph\]](#).
 - [106] M. Son and A. Urbano, “A new scalar resonance at 750 GeV: Towards a proof of concept

- in favor of strongly interacting theories,” [arXiv:1512.08307 \[hep-ph\]](#).
- [107] Y.-L. Tang and S.-h. Zhu, “NMSSM extended with vector-like particles and the diphoton excess on the LHC,” [arXiv:1512.08323 \[hep-ph\]](#).
 - [108] H. An, C. Cheung, and Y. Zhang, “Broad Diphotons from Narrow States,” [arXiv:1512.08378 \[hep-ph\]](#).
 - [109] J. Cao, F. Wang, and Y. Zhang, “Interpreting The 750 GeV Diphton Excess Within TopFlavor Seesaw Model,” [arXiv:1512.08392 \[hep-ph\]](#).
 - [110] F. Wang, W. Wang, L. Wu, J. M. Yang, and M. Zhang, “Interpreting 750 GeV Diphoton Resonance in the NMSSM with Vector-like Particles,” [arXiv:1512.08434 \[hep-ph\]](#).
 - [111] C. Cai, Z.-H. Yu, and H.-H. Zhang, “The 750 GeV diphoton resonance as a singlet scalar in an extra dimensional model,” [arXiv:1512.08440 \[hep-ph\]](#).
 - [112] Q.-H. Cao, Y. Liu, K.-P. Xie, B. Yan, and D.-M. Zhang, “The Diphoton Excess, Low Energy Theorem and the 331 Model,” [arXiv:1512.08441 \[hep-ph\]](#).
 - [113] J. E. Kim, “Is an axizilla possible for di-photon resonance?,” [arXiv:1512.08467 \[hep-ph\]](#).
 - [114] J. Gao, H. Zhang, and H. X. Zhu, “Diphoton excess at 750 GeV: gluon-gluon fusion or quark-antiquark annihilation?,” [arXiv:1512.08478 \[hep-ph\]](#).
 - [115] W. Chao, “Neutrino Catalyzed Diphoton Excess,” [arXiv:1512.08484 \[hep-ph\]](#).
 - [116] X.-J. Bi, R. Ding, Y. Fan, L. Huang, C. Li, T. Li, S. Raza, X.-C. Wang, and B. Zhu, “A Promising Interpretation of Diphoton Resonance at 750 GeV,” [arXiv:1512.08497 \[hep-ph\]](#).
 - [117] F. Goertz, J. F. Kamenik, A. Katz, and M. Nardecchia, “Indirect Constraints on the Scalar Di-Photon Resonance at the LHC,” [arXiv:1512.08500 \[hep-ph\]](#).
 - [118] L. A. Anchordoqui, I. Antoniadis, H. Goldberg, X. Huang, D. Lust, and T. R. Taylor, “750 GeV diphotons from closed string states,” [arXiv:1512.08502 \[hep-ph\]](#).
 - [119] P. S. B. Dev, R. N. Mohapatra, and Y. Zhang, “Quark Seesaw Vectorlike Fermions and Diphoton Excess,” [arXiv:1512.08507 \[hep-ph\]](#).
 - [120] N. Bizot, S. Davidson, M. Frigerio, and J. L. Kneur, “Two Higgs doublets to explain the excesses $pp \rightarrow \gamma\gamma(750 \text{ GeV})$ and $h \rightarrow \tau^\pm \mu^\mp$,” [arXiv:1512.08508 \[hep-ph\]](#).
 - [121] **ATLAS** Collaboration, G. Aad *et al.*, “Search for high-mass diphoton resonances in pp collisions at $\sqrt{s} = 8 \text{ TeV}$ with the ATLAS detector,” *Phys. Rev.* **D92** no. 3, (2015) 032004, [arXiv:1504.05511 \[hep-ex\]](#).
 - [122] **CMS** Collaboration, “Search for new resonances in the diphoton final state in the range between 150 and 850 GeV in pp collisions at $\sqrt{s} = 8 \text{ TeV}$,” Tech. Rep. CMS-PAS-HIG-14-006, CERN, Geneva, 2014.
 - [123] “<https://twiki.cern.ch/twiki/bin/view/lhcphysics/cernyellowreportpageat1314tev>.”
 - [124] **LHC Higgs Cross Section Working Group** Collaboration, J. R. Andersen *et al.*, “Handbook of LHC Higgs Cross Sections: 3. Higgs Properties,” [arXiv:1307.1347 \[hep-ph\]](#).
 - [125] **ATLAS** Collaboration, G. Aad *et al.*, “Search for an additional, heavy Higgs boson in the $H \rightarrow ZZ$ decay channel at $\sqrt{s} = 8 \text{ TeV}$ in pp collision data with the ATLAS detector,” [arXiv:1507.05930 \[hep-ex\]](#).
 - [126] **CMS** Collaboration, V. Khachatryan *et al.*, “Search for a Higgs Boson in the Mass Range from 145 to 1000 GeV Decaying to a Pair of W or Z Bosons,” *JHEP* **10** (2015) 144, [arXiv:1504.00936 \[hep-ex\]](#).
 - [127] A. Zee, “A Theory of Lepton Number Violation, Neutrino Majorana Mass, and

- Oscillation,” *Phys. Lett.* **B93** (1980) 389. [Erratum: *Phys. Lett.*B95,461(1980)].
- [128] T. P. Cheng and L.-F. Li, “Neutrino Masses, Mixings and Oscillations in $SU(2) \times U(1)$ Models of Electroweak Interactions,” *Phys. Rev.* **D22** (1980) 2860.
 - [129] A. Zee, “Quantum Numbers of Majorana Neutrino Masses,” *Nucl. Phys.* **B264** (1986) 99.
 - [130] K. S. Babu, “Model of ‘Calculable’ Majorana Neutrino Masses,” *Phys. Lett.* **B203** (1988) 132.
 - [131] E. Ma, “Verifiable radiative seesaw mechanism of neutrino mass and dark matter,” *Phys. Rev.* **D73** (2006) 077301, [arXiv:hep-ph/0601225](#) [[hep-ph](#)].
 - [132] L. M. Krauss, S. Nasri, and M. Trodden, “A Model for neutrino masses and dark matter,” *Phys. Rev.* **D67** (2003) 085002, [arXiv:hep-ph/0210389](#) [[hep-ph](#)].
 - [133] M. Aoki, S. Kanemura, and O. Seto, “Neutrino mass, Dark Matter and Baryon Asymmetry via TeV-Scale Physics without Fine-Tuning,” *Phys. Rev. Lett.* **102** (2009) 051805, [arXiv:0807.0361](#) [[hep-ph](#)].
 - [134] M. Aoki, S. Kanemura, and K. Yagyu, “Triviality and vacuum stability bounds in the three-loop neutrino mass model,” *Phys. Rev.* **D83** (2011) 075016, [arXiv:1102.3412](#) [[hep-ph](#)].
 - [135] M. Gustafsson, J. M. No, and M. A. Rivera, “Predictive Model for Radiatively Induced Neutrino Masses and Mixings with Dark Matter,” *Phys. Rev. Lett.* **110** no. 21, (2013) 211802, [arXiv:1212.4806](#) [[hep-ph](#)]. [Erratum: *Phys. Rev. Lett.*112,no.25,259902(2014)].
 - [136] Y. Kajiyama, H. Okada, and K. Yagyu, “ T_7 Flavor Model in Three Loop Seesaw and Higgs Phenomenology,” *JHEP* **10** (2013) 196, [arXiv:1307.0480](#) [[hep-ph](#)].
 - [137] A. Ahriche, C.-S. Chen, K. L. McDonald, and S. Nasri, “Three-loop model of neutrino mass with dark matter,” *Phys. Rev.* **D90** (2014) 015024, [arXiv:1404.2696](#) [[hep-ph](#)].
 - [138] A. Ahriche, K. L. McDonald, and S. Nasri, “A Model of Radiative Neutrino Mass: with or without Dark Matter,” *JHEP* **10** (2014) 167, [arXiv:1404.5917](#) [[hep-ph](#)].
 - [139] C.-S. Chen, K. L. McDonald, and S. Nasri, “A Class of Three-Loop Models with Neutrino Mass and Dark Matter,” *Phys. Lett.* **B734** (2014) 388–393, [arXiv:1404.6033](#) [[hep-ph](#)].
 - [140] H. Okada and Y. Orikasa, “X-ray line in Radiative Neutrino Model with Global $U(1)$ Symmetry,” *Phys. Rev.* **D90** no. 7, (2014) 075023, [arXiv:1407.2543](#) [[hep-ph](#)].
 - [141] H. Hatanaka, K. Nishiwaki, H. Okada, and Y. Orikasa, “A Three-Loop Neutrino Model with Global $U(1)$ Symmetry,” *Nucl. Phys.* **B894** (2015) 268–283, [arXiv:1412.8664](#) [[hep-ph](#)].
 - [142] L.-G. Jin, R. Tang, and F. Zhang, “A three-loop radiative neutrino mass model with dark matter,” *Phys. Lett.* **B741** (2015) 163–167, [arXiv:1501.02020](#) [[hep-ph](#)].
 - [143] P. Culjak, K. Kumericki, and I. Picek, “Scotogenic $R\nu$ MDM at three-loop level,” *Phys. Lett.* **B744** (2015) 237–243, [arXiv:1502.07887](#) [[hep-ph](#)].
 - [144] C.-Q. Geng, D. Huang, and L.-H. Tsai, “Comment on ”A three-loop radiative neutrino mass model with dark matter” [*Phys. Lett. B* 741 (2015) 163],” *Phys. Lett.* **B745** (2015) 56–57, [arXiv:1504.05468](#) [[hep-ph](#)].
 - [145] A. Ahriche, K. L. McDonald, S. Nasri, and T. Toma, “A Model of Neutrino Mass and Dark Matter with an Accidental Symmetry,” *Phys. Lett.* **B746** (2015) 430–435, [arXiv:1504.05755](#) [[hep-ph](#)].
 - [146] K. Nishiwaki, H. Okada, and Y. Orikasa, “Three loop neutrino model with isolated $k^{\pm\pm}$,” *Phys. Rev.* **D92** no. 9, (2015) 093013, [arXiv:1507.02412](#) [[hep-ph](#)].

- [147] H. Okada and K. Yagyu, “Three-loop Neutrino Mass Model with Doubly Charged Particles from Iso-Doublets,” [arXiv:1508.01046 \[hep-ph\]](#).
- [148] A. Ahriche, K. L. McDonald, and S. Nasri, “A Radiative Model for the Weak Scale and Neutrino Mass via Dark Matter,” [arXiv:1508.02607 \[hep-ph\]](#).
- [149] A. Ahriche, K. L. McDonald, and S. Nasri, “Scalar Sector Phenomenology of Three-Loop Radiative Neutrino Mass Models,” *Phys. Rev.* **D92** no. 9, (2015) 095020, [arXiv:1508.05881 \[hep-ph\]](#).
- [150] S. C. Park and J. Shu, “Split Universal Extra Dimensions and Dark Matter,” *Phys. Rev.* **D79** (2009) 091702, [arXiv:0901.0720 \[hep-ph\]](#).
- [151] C.-R. Chen, M. M. Nojiri, S. C. Park, J. Shu, and M. Takeuchi, “Dark matter and collider phenomenology of split-UED,” *JHEP* **09** (2009) 078, [arXiv:0903.1971 \[hep-ph\]](#).
- [152] C.-R. Chen, M. M. Nojiri, S. C. Park, and J. Shu, “Kaluza-Klein Dark Matter After Fermi,” [arXiv:0908.4317 \[hep-ph\]](#).
- [153] S. C. Park and J. Shu, “Dark Matter and Collider Physics in Split-UED,” *AIP Conf. Proc.* **1200** (2010) 587–590, [arXiv:0910.0931 \[hep-ph\]](#). [AIP Conf. Proc.1200,1051(2010)].
- [154] K. Kong, S. C. Park, and T. G. Rizzo, “Collider Phenomenology with Split-UED,” *JHEP* **04** (2010) 081, [arXiv:1002.0602 \[hep-ph\]](#).
- [155] K. Kong, S. C. Park, and T. G. Rizzo, “A vector-like fourth generation with a discrete symmetry from Split-UED,” *JHEP* **07** (2010) 059, [arXiv:1004.4635 \[hep-ph\]](#).
- [156] C. Csaki, J. Heinonen, J. Hubisz, S. C. Park, and J. Shu, “5D UED: Flat and Flavorless,” *JHEP* **01** (2011) 089, [arXiv:1007.0025 \[hep-ph\]](#).
- [157] K. Nishiwaki, “Higgs production and decay processes via loop diagrams in various 6D Universal Extra Dimension Models at LHC,” *JHEP* **05** (2012) 111, [arXiv:1101.0649 \[hep-ph\]](#).
- [158] K. Nishiwaki, K.-y. Oda, N. Okuda, and R. Watanabe, “A Bound on Universal Extra Dimension Models from up to 2 fb^{-1} of LHC Data at 7TeV,” *Phys. Lett.* **B707** (2012) 506–511, [arXiv:1108.1764 \[hep-ph\]](#).
- [159] K. Nishiwaki, K.-y. Oda, N. Okuda, and R. Watanabe, “Heavy Higgs at Tevatron and LHC in Universal Extra Dimension Models,” *Phys. Rev.* **D85** (2012) 035026, [arXiv:1108.1765 \[hep-ph\]](#).
- [160] D. Kim, Y. Oh, and S. C. Park, “ W' at the LHC with $\sqrt{s} = 14\text{ TeV}$: Split universal extra dimension model,” *J. Korean Phys. Soc.* **67** (2015) 1137–1141, [arXiv:1109.1870 \[hep-ph\]](#).
- [161] A. Datta, K. Nishiwaki, and S. Niyogi, “Non-minimal Universal Extra Dimensions: The Strongly Interacting Sector at the Large Hadron Collider,” *JHEP* **11** (2012) 154, [arXiv:1206.3987 \[hep-ph\]](#).
- [162] T. Flacke, K. Kong, and S. C. Park, “Phenomenology of Universal Extra Dimensions with Bulk-Masses and Brane-Localized Terms,” *JHEP* **05** (2013) 111, [arXiv:1303.0872 \[hep-ph\]](#).
- [163] T. Kakuda, K. Nishiwaki, K.-y. Oda, and R. Watanabe, “Universal extra dimensions after Higgs discovery,” *Phys. Rev.* **D88** (2013) 035007, [arXiv:1305.1686 \[hep-ph\]](#).
- [164] T. Flacke, K. Kong, and S. C. Park, “126 GeV Higgs in Next-to-Minimal Universal Extra Dimensions,” *Phys. Lett.* **B728** (2014) 262–267, [arXiv:1309.7077 \[hep-ph\]](#).
- [165] A. Datta, K. Nishiwaki, and S. Niyogi, “Non-minimal Universal Extra Dimensions with

- Brane Local Terms: The Top Quark Sector,” *JHEP* **01** (2014) 104, [arXiv:1310.6994 \[hep-ph\]](#).
- [166] H. Dohi, T. Kakuda, K. Nishiwaki, K.-y. Oda, and N. Okuda, “Notes on sphere-based universal extra dimensions,” *Afr. Rev. Phys.* **9** (2014) 0069, [arXiv:1406.1954 \[hep-ph\]](#).
 - [167] T. Flacke, K. Kong, and S. C. Park, “A Review on Non-Minimal Universal Extra Dimensions,” *Mod. Phys. Lett.* **A30** no. 05, (2015) 1530003, [arXiv:1408.4024 \[hep-ph\]](#).
 - [168] H. M. Lee, D. Kim, K. Kong, and S. C. Park, “Diboson Excesses Demystified in Effective Field Theory Approach,” *JHEP* **11** (2015) 150, [arXiv:1507.06312 \[hep-ph\]](#).
 - [169] J. R. Ellis, M. K. Gaillard, and D. V. Nanopoulos, “A Phenomenological Profile of the Higgs Boson,” *Nucl. Phys.* **B106** (1976) 292.
 - [170] M. A. Shifman, A. I. Vainshtein, M. B. Voloshin, and V. I. Zakharov, “Low-Energy Theorems for Higgs Boson Couplings to Photons,” *Sov. J. Nucl. Phys.* **30** (1979) 711–716. [*Yad. Fiz.*30,1368(1979)].
 - [171] A. Djouadi, “The Anatomy of electro-weak symmetry breaking. I: The Higgs boson in the standard model,” *Phys. Rept.* **457** (2008) 1–216, [arXiv:hep-ph/0503172 \[hep-ph\]](#).
 - [172] M. Carena, I. Low, and C. E. M. Wagner, “Implications of a Modified Higgs to Diphoton Decay Width,” *JHEP* **08** (2012) 060, [arXiv:1206.1082 \[hep-ph\]](#).
 - [173] C.-S. Chen, C.-Q. Geng, D. Huang, and L.-H. Tsai, “New Scalar Contributions to $h \rightarrow Z\gamma$,” *Phys. Rev.* **D87** (2013) 075019, [arXiv:1301.4694 \[hep-ph\]](#).
 - [174] C. F. von Weizsacker, “Radiation emitted in collisions of very fast electrons,” *Z. Phys.* **88** (1934) 612–625.
 - [175] E. J. Williams, “Nature of the high-energy particles of penetrating radiation and status of ionization and radiation formulae,” *Phys. Rev.* **45** (1934) 729–730.
 - [176] V. M. Budnev, I. F. Ginzburg, G. V. Meledin, and V. G. Serbo, “The Two photon particle production mechanism. Physical problems. Applications. Equivalent photon approximation,” *Phys. Rept.* **15** (1975) 181–281.
 - [177] A. D. Martin and M. G. Ryskin, “The photon PDF of the proton,” *Eur. Phys. J.* **C74** (2014) 3040, [arXiv:1406.2118 \[hep-ph\]](#).
 - [178] **Particle Data Group** Collaboration, K. A. Olive *et al.*, “Review of Particle Physics,” *Chin. Phys.* **C38** (2014) 090001.
 - [179] **ATLAS** Collaboration, G. Aad *et al.*, “Search for anomalous production of prompt same-sign lepton pairs and pair-produced doubly charged Higgs bosons with $\sqrt{s} = 8$ TeV pp collisions using the ATLAS detector,” *JHEP* **03** (2015) 041, [arXiv:1412.0237 \[hep-ex\]](#).
 - [180] **ATLAS** Collaboration, G. Aad *et al.*, “Search for new resonances in $W\gamma$ and $Z\gamma$ final states in pp collisions at $\sqrt{s} = 8$ TeV with the ATLAS detector,” *Phys. Lett.* **B738** (2014) 428–447, [arXiv:1407.8150 \[hep-ex\]](#).
 - [181] A. Schuessler and D. Zeppenfeld, “Unitarity constraints on MSSM trilinear couplings,” in *SUSY 2007 proceedings, 15th International Conference on Supersymmetry and Unification of Fundamental Interactions, July 26 - August 1, 2007, Karlsruhe, Germany*. 2007. [arXiv:0710.5175 \[hep-ph\]](#).
 - [182] J. Alwall, R. Frederix, S. Frixione, V. Hirschi, F. Maltoni, O. Mattelaer, H. S. Shao, T. Stelzer, P. Torrielli, and M. Zaro, “The automated computation of tree-level and next-to-leading order differential cross sections, and their matching to parton shower simulations,” *JHEP* **07** (2014) 079, [arXiv:1405.0301 \[hep-ph\]](#).
 - [183] A. Alloul, N. D. Christensen, C. Degrande, C. Duhr, and B. Fuks, “FeynRules 2.0 - A

- complete toolbox for tree-level phenomenology,”
Comput. Phys. Commun. **185** (2014) 2250–2300, [arXiv:1310.1921 \[hep-ph\]](#).
- [184] J. Pumplin, D. R. Stump, J. Huston, H. L. Lai, P. M. Nadolsky, and W. K. Tung, “New generation of parton distributions with uncertainties from global QCD analysis,” *JHEP* **07** (2002) 012, [arXiv:hep-ph/0201195 \[hep-ph\]](#).
 - [185] S. Kanemura, Y. Okada, and E. Senaha, “Electroweak baryogenesis and quantum corrections to the triple Higgs boson coupling,” *Phys. Lett.* **B606** (2005) 361–366, [arXiv:hep-ph/0411354 \[hep-ph\]](#).
 - [186] **ATLAS** Collaboration, G. Aad *et al.*, “Measurement of Higgs boson production in the diphoton decay channel in pp collisions at center-of-mass energies of 7 and 8 TeV with the ATLAS detector,” *Phys. Rev.* **D90** no. 11, (2014) 112015, [arXiv:1408.7084 \[hep-ex\]](#).
 - [187] **ATLAS** Collaboration, G. Aad *et al.*, “Measurements of Higgs boson production and couplings in the four-lepton channel in pp collisions at center-of-mass energies of 7 and 8 TeV with the ATLAS detector,” *Phys. Rev.* **D91** no. 1, (2015) 012006, [arXiv:1408.5191 \[hep-ex\]](#).
 - [188] **ATLAS** Collaboration, G. Aad *et al.*, “Observation and measurement of Higgs boson decays to WW^* with the ATLAS detector,” *Phys. Rev.* **D92** no. 1, (2015) 012006, [arXiv:1412.2641 \[hep-ex\]](#).
 - [189] **ATLAS** Collaboration, G. Aad *et al.*, “Search for the $b\bar{b}$ decay of the Standard Model Higgs boson in associated $(W/Z)H$ production with the ATLAS detector,” *JHEP* **01** (2015) 069, [arXiv:1409.6212 \[hep-ex\]](#).
 - [190] “Evidence for Higgs boson Yukawa couplings in the $H \rightarrow \tau\tau$ decay mode with the ATLAS detector,” Tech. Rep. ATLAS-CONF-2014-061, CERN, Geneva, Oct, 2014.
 - [191] **CMS** Collaboration, V. Khachatryan *et al.*, “Precise determination of the mass of the Higgs boson and tests of compatibility of its couplings with the standard model predictions using proton collisions at 7 and 8 TeV,” *Eur. Phys. J.* **C75** no. 5, (2015) 212, [arXiv:1412.8662 \[hep-ex\]](#).